Supporting information for

Target-Activated Modulation of Dual-Color and Two-Photon Fluorescence of Graphene Quantum Dots for *in Vivo* Imaging of Hydrogen Peroxide

Wenjie Zhao,[†,§] Yinhui Li,[†,§] Sheng Yang,[‡,*] Yun Chen,[†] Jing Zheng,[†] Changhui Liu,[†] Zhihe Qing,[‡] Jishan Li,[†] and Ronghua Yang[†,‡,*]

[†]State Key Laboratory of Chemo/Biosensing and Chemometrics, College of Chemistry and Chemical Engineering, and Collaborative Innovation Center for Chemistry and Molecular Medicine, Hunan University, Changsha, 410082, P. R. China; [‡]School of Chemistry and Biological Engineering, Changsha University of Science and Technology, Changsha 410004, P. R. China.

[§]These authors contributed equally.

*To whom correspondence should be addressed:

E-mail: Yangrh@pku.edu.cn; ysh1127@hnu.edu.cn

Fax: +86-731-8882 2523

Contents

Materials and Instruments

All the chemical reagents were purchased from Alfa Aesar. The reactive oxygen species (ROS) were prepared following reported literature.[1] The graphene oxide (GO) used in this work was purchased from XFNANO Materials Tech Co., Ltd. (China). Working solutions were prepared by successive dilution of the stock solution with PBS buffer (20 mM, 10% DMF, pH 7.4).

UV-Vis absorption spectra were recorded using a Hitachi U-4100 UV/Vis spectrophotometer (Kyoto, Japan) in 1 cm path length quartz cuvettes. The steady-state fluorescence emission spectra were obtained from a was measured on a Photon Technology Intl. Fluorescence emission spectra were collected using a bandwidth of 5 nm and 0.5 × 1 cm^2 quartz cuvettes containing 500 μL of solution. AFM images were obtained using a Nanoscope IIIa apparatus (Digital Instruments, USA) equipped with a J Scanner. Transmission electron microscopy (TEM) images were obtained on an H-7000 NAR transmission electron microscope (Hitachi) with a working voltage of 100 kV. ^{1}H and ^{13}C NMR spectra were recorded on an Invoa-400 (Invoa 400) spectrometer and referenced to solvent signals. Mass spectra were measured on LCQ/Advantage HPLC-Mass spectrotometer. X-ray photoelectron spectroscopy (XPS) (model K-Alpha 1063, Thermo Fisher Scientific, UK) equipped with Al K source (1486.6 eV photons) was used to track the assembly process of the probe. All binding energies (BEs) were referred to as the C1s peak (284.6 eV) arising from surface hydrocarbons. The fluorescence images were acquired from the blue channel (400-450 nm) and green channel (500-550 nm) upon two-photon excitation at 740 nm with a pulse laser by using an Olympus FV1000 laser confocal microscope.

Synthesis of TPGQD^{420}

In brief the graphene oxide (GO) was dissolved in dimethylformamide (DMF) with a concentration of ~200 mg mL^{-1}. The GO and DMF mixed solution was ultrasonicated for 30 minutes (120 W, 100 kHz) and then transferred to a poly(tetrafluoroethylene)-lined autoclave (30 mL) and heated at 200□ for 5 h. After cooling to room temperature naturally, the obtained mixture was filtered through a 0.22 μm microporous membrane to remove the black precipitates, obtaining a brown solution. The solvent was removed with the aid of a rotary evaporator. Then obtained TPGQD^{420} was dispersed in DI water. The product dialyzed through a 3.5 KDa dialyzer for at least 48 hours. Then obtained pure TPGQD^{420} used for further characterization.

Spectral Measurements

The BMC1-4, BMC3-COOH, and TPGQD^{420}-BMC3 were used to prepare stock solutions in Millipore water. Test solutions were prepared by placing TPGQD^{420}-BMC3 an appropriate aliquot of each analyte stock into a flask and then diluting the solution to a volume of 500 mL with 20mM PBS, pH 7.4 (containing 10 % DMF).The resulting solution was kept at ambient temperature for 30 min, and then the fluorescence intensities were recorded with two-photon excitation at 740 nm. In kinetic studies, the apparent rate constant k for the reaction of BMC1-4 with H_2O_2 were determined by fitting the absorbance intensities to the pseudo first-order:

$$\ln[|(A_{max} - A_t)|/A_{max}] = -kt^{2}$$

Where A_t and A_{max} are the absorbance intensities of BMC1-4 at a time t and the maximum value obtained after the reaction was complete.

The observed rate constant k', contains the concentration of H_2O_2 as a constant and is

related to the second-order rate constant, k ($M^{-1}s^{-1}$), by equation:

$$k' = k[H_2O_2]$$

DFT Calculations:[3]

The ground state structures of dyes BMC1-4 were optimized using DFT with B3LYP functional and 6-31+G (d, p) basis set. The initial geometries of the compounds were generated by the GaussView software. All of these calculations were performed with Gaussian 09 (Revision A.02).

Measurements of One-photon Quantum Yields and Two-Photon Absorbance Cross Section

The one-photon quantum yields (QY) of samples were estimated using Rhodamine B or quinine sulfate as a reference standard, which was freshly prepared to reduce the measurement error.[4] The quantum yield $\boldsymbol{\Phi}$ as a function solvent polarity is calculated using the following equation:

$$\Phi_F = \Phi_{F,\mathrm{cal}} \cdot \frac{S}{S_{cal}} \cdot \frac{A_{cal}}{A} \cdot \frac{n^2}{n^2_{cal}}$$

Where $\boldsymbol{\Phi}_F$ is the quantum yield, $\boldsymbol{S}$ is the areas' integral values of the corrected fluorescence spectra, $\boldsymbol{A}$ stands for the absorbance and $\boldsymbol{n}$ is refractive index. The subscript cal and no denote the standard and sample, respectively.

The two-photon absorption (TPA) cross sections ($\boldsymbol{\delta}$) of samples (in the wavelength range of 690-860 nm) in neutral conditions were determined using TPE method with femtosecond Ti-sapphire laser pulses described in previous literature.[5] $TPGQD^{420}$ (1.46 μg/mL) or BMC 1-4 (10 μM) was dissolved in PBS buffer (pH 7.4), and the TPE fluorescence emission intensity was measured in the emission range 380-450 nm under excitation at 690-860

nmusing Rhodamine B as the reference, whose TP properties have been well-characterized in the previous literature.[6] Intensities of TPE fluorescence emission of the reference and the samples emitted at the same excitation wavelength were determined. The TPA cross section was calculated as the following equation: [7, 8]

$$\delta_S = \frac{S_S}{S_R} \cdot \left[\frac{\Phi_R \cdot C_R \cdot n_S}{\Phi_S \cdot C_S \cdot n_R} \right] \delta_R$$

Subscript ***S*** and ***R*** denote the sample and the reference, respectively. ***S*** represents the intensity of TPE fluorescence emission, ***Φ*** is the fluorescence quantum yield, ***C*** denotes the concentration, and ***n*** represents the refractive index of the solvents.

Cell Incubation and Cytotoxicity Assay

HeLa cells were obtained from the biomedical engineering center of Hunan University (Changsha, China). Those cell was cultured using high-glucose Dulbecco's modified Eagle's medium (DMEM, GIBCO) with 1% penicillin-streptomycin (10,000 U/mL, 10,000 μg mL^{-1}, Invitrogen) and 10% fatal bovine serum (GIBCO) in an atmosphere of 5% CO_2 and 95% air at 37℃.

The cellular cytotoxicity of $TPGQD^{420}$-BMC3@PEG towards HeLa cells as the model was evaluated using the standard cell viability assay - the MTT assay.[9] HeLa cells were seeded into a 96-well plate at a concentration of 5×10^3 cells $well^{-1}$ in 100 μL of DMEM medium with 10% FBS. Plates were maintained at 37 ℃ in a 5% CO_2 95% air incubator for 24 h. After the original medium was removed, the HeLa cells were incubated with $TPGQD^{420}$-BMC3@PEG with different concentration (0, 5, 10, 20, and 50 μg mL^{-1}). The cells incubated with the culture medium only were served as the controls. The cells were washed with PBS for three

times and then 100 μL MTT solution (0.5 mg mL^{-1} in PBS) was added to each well. After addition of DMSO (150 μL $well^{-1}$), the assay plate was allowed to shake at room temperature for 10 min. The spectrophotometrical absorbance of the samples was measured by using a Tecan microplate (ELISA) reader. The cell viability was calculated based on measuring the UV-vis absorption at 570 nm using the following equation, where OD_{570} represents the optical density.[10]

$$\text{Cell viability} = [OD_{570(\text{sample})} - OD_{570(\text{blank})}] / [OD_{570(\text{control})} - OD_{570(\text{blank})}]$$

Mice Culture and Preparation of Tumor Tissue Slices

Eight-week-old BALB/c nude mice (male) purchased from SJA Co., Ltd. (Changsha, China) were used as in vivo imaging mode and the previous procedure of cervical tumor tissue slices preparation. All animal operations were in accord with institutional animal use and care regulations, according to protocol No. SYXK (Xiang) 2008-0001, approved by Laboratory Animal Center of Hunan. Preparation of cervical tumor tissue slices follow the previous procedure: a total of 2×10^6 HeLa cells diluted in 100 μL of serum-free DMEM medium were injected subcutaneously into the right flank of 6 to 8-week-old BALB/c nude mice to inoculate tumors. After inoculation for 15-20 days, mice were sacrificed. Tumors were transferred and embedded with O.C.T (Sakura Finetek, USA, Torrance, CA) for frozen sections. The tissues were cut into 10 μm thick slices using a vibrating-blade microtome.

References

(1) Yuan, L.; Lin, W.; Zhao, S. *J. Am. Chem. Soc*. **2012**, *134*, 13510-13523.

(2) Dale, T. J.; Rebek, J. *J. Am. Chem. Soc*. **2006**, *128*, 4500-4501.

(3) Frisch, M. J.; Trucks, G. W.; Schlegel, H. B.; Scuseria, G. E.; Robb, M. A.; Cheeseman, J.

R.; Scalmani, G.; Barone, V.; Mennucci, B.; Petersson, G. A.; Nakatsuji, H.; Caricato, M.; Li, X.; Hratchian, H. P.; Izmaylov, A. F.; Bloino, J.; Zheng, G.; Sonnenberg, J. L.; Hada, M.; Ehara, M.; Toyota, K.; Fukuda, R.; Hasegawa, J.; Ishida, M.; Nakajima, T.; Honda, Y.; Kitao, O.; Nakai, H.; Vreven, T.; Montgomery, J. A.; Peralta, J. E.; Ogliaro, F.; Bearpark, M.; Heyd, J. J.; Brothers, E.; Kudin, K. N.; Staroverov, V. N.; Kobayashi, R.; Normand, J.; Raghavachari, K.; Rendell, A.; Burant, J. C.; Iyengar, S. S.; Tomasi, J.; Cossi, M.; Rega, N.; Millam, J. M.; Klene, M.; Knox, J. E.; Cross, J. B.; Bakken, V.; Adamo, C.; Jaramillo, J.; Gomperts, R.; Stratmann, R. E.; Yazyev, O.; Austin, A. J.; Cammi, R.; Pomelli, C.; Ochterski, J. W.; Martin, R. L.; Morokuma, K.; Zakrzewski, V. G.; Voth, G. A.; Salvador, P.; Dannenberg, J. J.; Dapprich, S.; Daniels, A. D.; Farkas, O.; Foresman, J. B.; Ortiz, J. V.; Cioslowski, J.; Fox, D. J. Gaussian, Inc., Wallingford CT, GAUSSIAN 09 (Revision A.02), Gaussian, Inc., Pittsburgh, PA, 2009.

(4) Demasa, J. ; Crosby, G. A. *J. Phys. Chem*. **1971**, *75*, 991-1024.

(5) Lee, S.; Yang,W.; Choi,J.; Kim,C.; Jeon, S.; Cho,B. *Org. Lett.* **2005**, 7, 323-326.

(6)Makarov,N.; Drobizhev, M.; Rebane,A. *Opt. Express.* **2008**, *16*, 4029-4047.

(7) Xu, C.; Webb, W. *J. Opt. Soc. Am. B*. **1996**, *13*, 481-491.

(8) Rumi, M.; Ehrlich,J.; Heikal,A.; Perry,J.; Barlow, S.; Hu, Z.; McCord-Maughon, D.; Parker, T.; Rockel, H.; Thayumanavan, S.; Marder, S.; Beljonne, D.; Bredas, J. *J. Am. Chem. Soc.* **2000**, *122*, 9500-9510.

(9) Mosmann, T. J. *Immunol. Methods.* **1983**, *65*, 55-63.

(10) Tang, J.; Kong, B.; Wu, H.; Xu, M.; Wang, Y.; Wang,Y.; Zhao, D.; Zheng, G.; *Adv. Mater.* **2013**, *25*, 6569-6574.

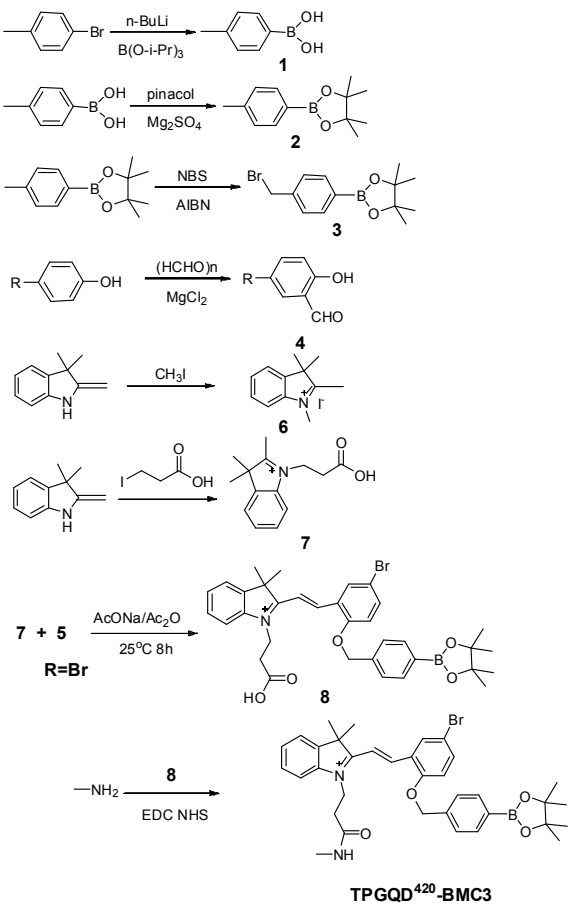

Scheme S1. Synthetic Routes of compounds 1-4, compounds 6-8 and TPGQD^{420}-BMC3.

Sample	-R	BDES, kJ·mol^{-1}	Bond-length, pm	$\Delta E_{(\text{LUMO-HOMO})}$, eV
BMC1	-H	236.38	146.07	2.5910
BMC2	-CF_3	213.14	146.45	2.4092
BMC3	-Br	223.43	146.30	2.5651
BMC4	-OCH_3	240.54	145.99	2.7960

Table S1. The CO−CH_2 Bond Lengths (in pm) Bond Dissociation Energies (BDES) (kJ·mol^{-1}) and $\Delta E_{(\text{LUMO-HOMO})}$ of BMC1-4 Determined by DFT Calculations.

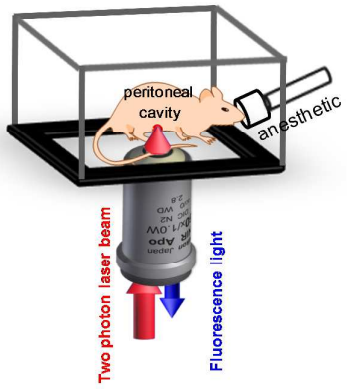

Figure S1. Schematic diagram of experimental set-up for *in vivo* ratiometric TPM images of endogenous H_2O_2 levels in inflamed mice.

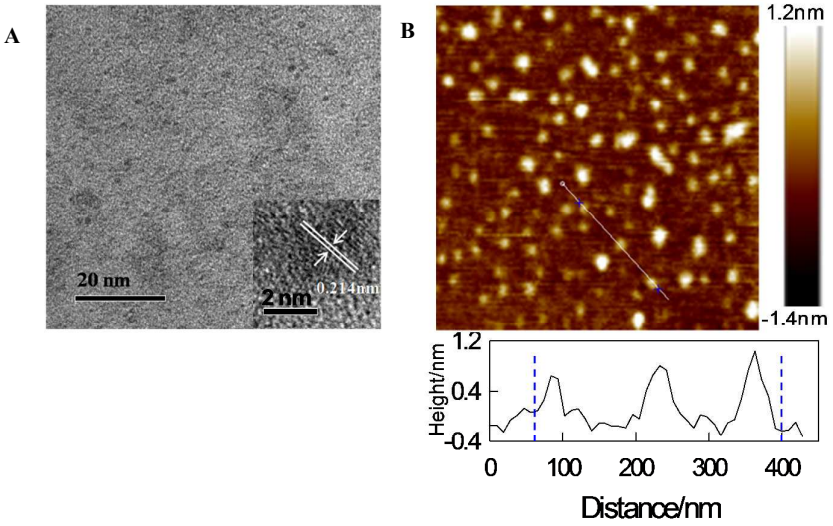

Figure S2. (A) TEM image of TPGQD^{420}. Inset: magnified images of TPGQD^{420}. (B) AFM topography image of TPGQD^{420} on mica substrates with the height profiles along the line in the image**.**

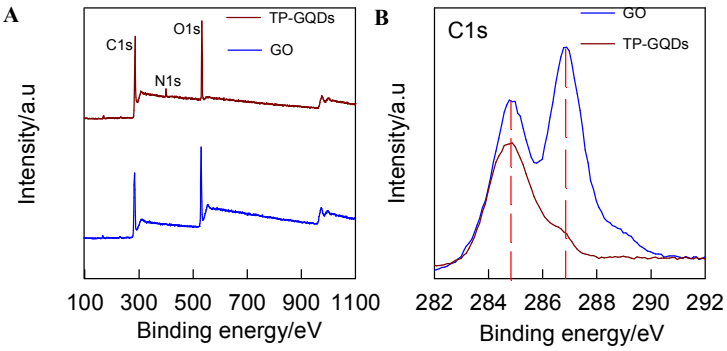

Figure S3. (A) XPS survey spectra of GO and TPGQD^{420}. (B) High-resolution C1s XPS

spectra of GO and TPGQD[420].

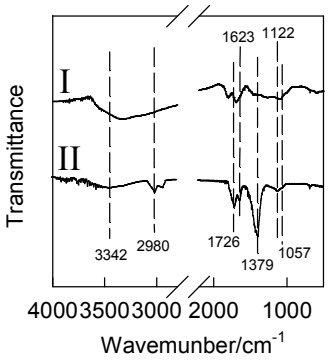

Figure S4. FT-IR spectra of (I) GO, (II) TPGQD[420].

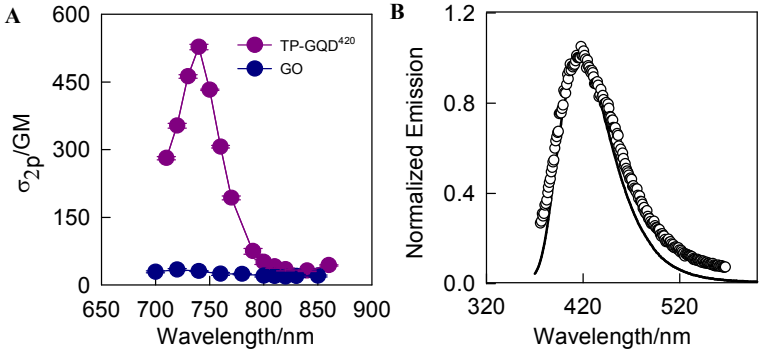

Figure S5. (A) Two-photon action cross sections of TPGQD[420] and GO. (B) One photon (solid line, λ_{ex} = 350 nm) and two-photon (circle, λ_{ex} = 740 nm) luminescence spectra of the TPGQD[420].

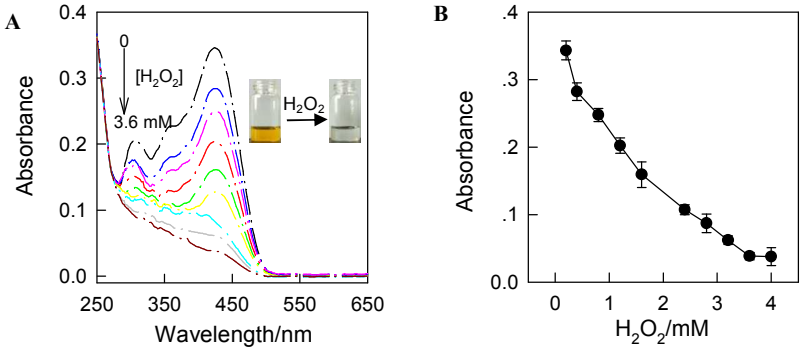

Figure S6. (A) UV−vis absorption spectra of 360 μM BMC3 in PBS buffer solution (pH 7.4) upon addition of different concentrations of H_2O_2. The down arrow indicates the signal

changes with the increases in H_2O_2 concentration (0, 0.4, 0.8, 1.2, 1.6, 1.8, 2.4, 2.8, 3.2, 3.6 mM). Inset: color change of BMC3 after treatment with H_2O_2. (B) The corresponding relationship between the maximum absorbance intensity and the H_2O_2 concentrations

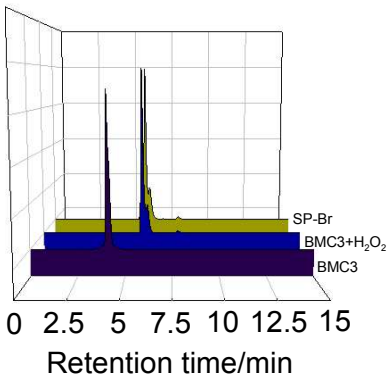

Figure S7. The reaction mechanism between BMC3 and H_2O_2 was verified by HPLC retention time detection. The product (SP-Br) of BMC3 (360μM) reaction with H_2O_2 (3.6mM) was determined. The retention time of the product (SP-Br) is 5.74 the same as the standard material Sp-Br.

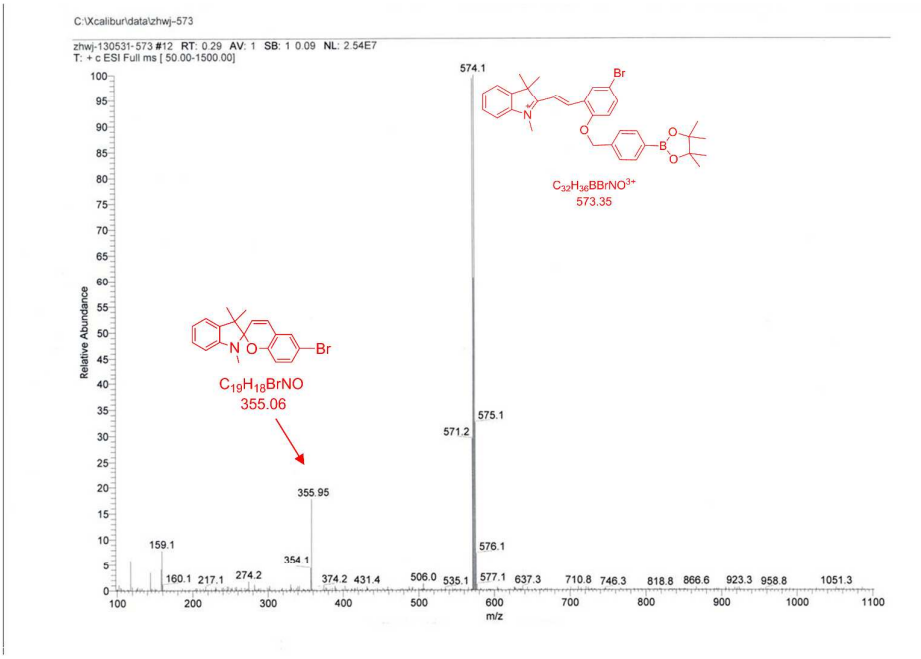

Figure S8. Mass spectrum of the product (SP-Br) of BMC3 reacted with H_2O_2.

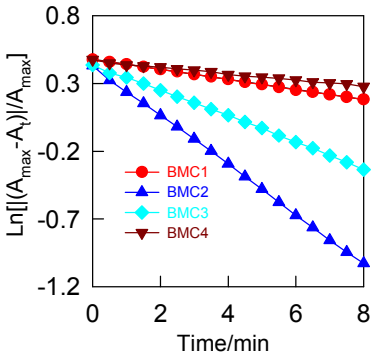

Figure S9. Kinetic plot of reaction of 360 μM BMC1-4 with 3.6 mM H_2O_2 in PBS buffer (20mM, 10% DMF, pH=7.4).

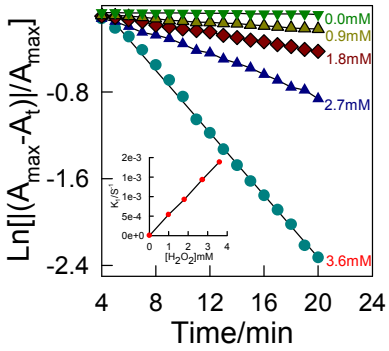

Figure S10. Plots of $Ln[|(A_{max}-A_t)|/A_{max}]$ vs time for the reaction of BMC3 with different concentrations H_2O_2 (0–3.6 mM) in PBS buffer (20 mM, 10% DMF, pH 7.4). Inset: Plot of k_1 vs concentration of H_2O_2.

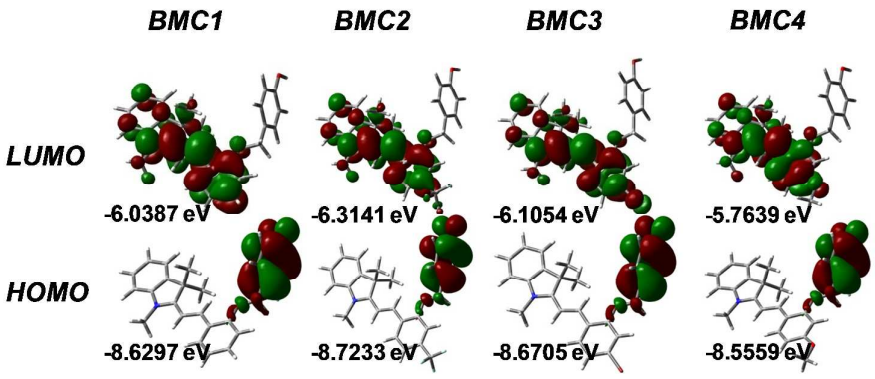

Figure S11. DFT optimized structures and molecular orbital plots (LUMO and HOMO) of BMC1-4 based on the optimized ground-state geometry. In the ball-and-stick representation, carbon, nitrogen, and oxygen atoms are colored in gray, blue, and red, respectively.

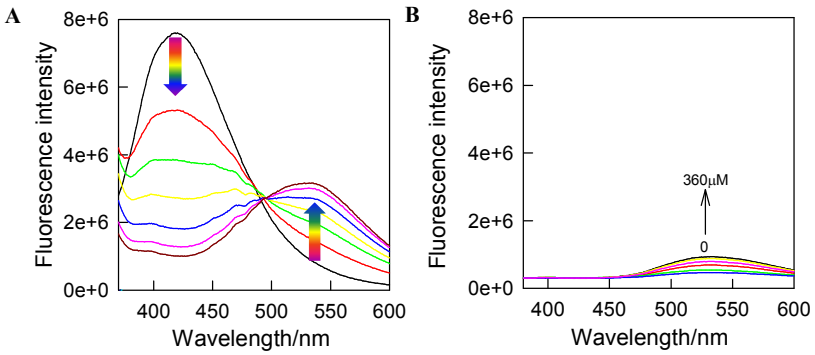

Figure S12. (A) Fluorescence emission changes of TPGQD^{420} (1.46 μg mL^{-1}) in PBS buffer solution (20mM, 10% DMF, pH 7.4) upon addition of different concentrations of BMC3. The arrows indicate the signal changes with increases in BMC3 concentrations (0, 60, 120, 180, 240, 300 and 360 μM). λ_{ex} = 350 nm. (B) Fluorescence intensity records in PBS buffer solution (20 mM, 10% DMF, pH 7.4) upon additions of different concentrations of BMC3 The arrow indicates the signal changes with increases in BMC3 concentrations (0, 60, 120, 180, 240, 300 and 360 μM). λ_{ex} = 350 nm.

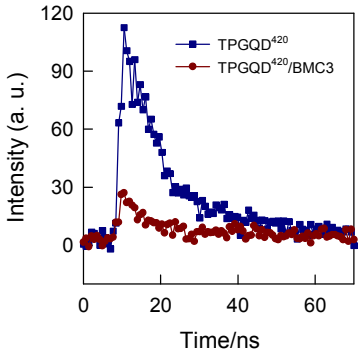

Figure S13. The time-resolved emission decays of TPGQD^{420} (1.46 μg mL-1) and TPGQD^{420}/BMC3 mixture (TPGQD^{420} (1.46 μg mL-1), BMC3 (360 μM)) in PBS buffer solution (20 mM, 10% DMF, pH 7.4). λex = 350 nm; λem = 420 nm.

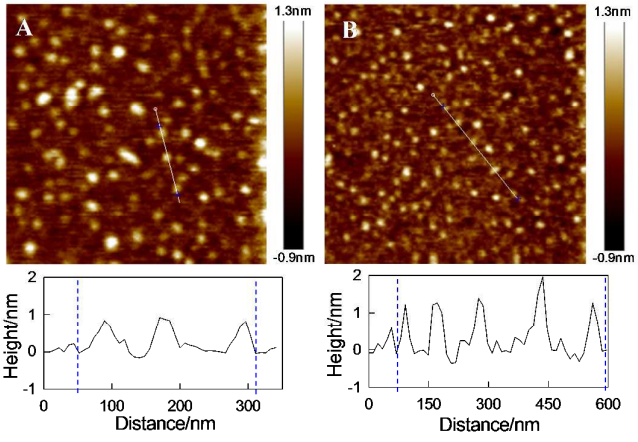

Figure S14. AFM images (top panel) acquired in air under tapping mode and the height profiles (down panel) of (A) TPGQD^{420} and (B) TPGQD^{420}-BMC3. Scale bar: 0.4 μm.

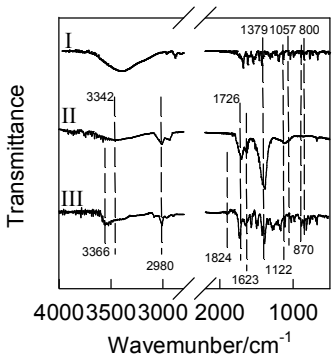

Figure S15. FT-IR spectra of (I) BMC3, (II) TPGQD^{420} and (III) TPGQD^{420}-BMC3 were compared each other.

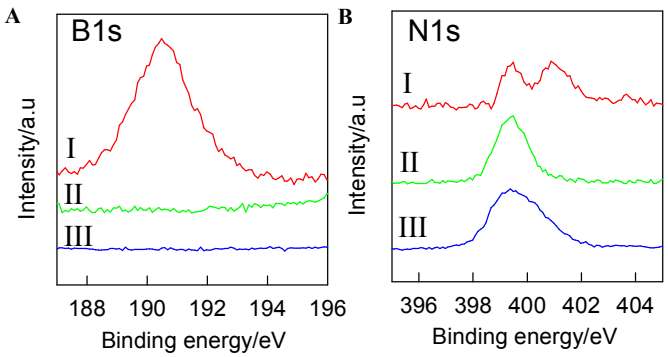

Figure S16. XPS spectra for (A) B 1s, (B) N 1s obtained at (I) TPGQD^{420}-BMC3, (II) TPGQD^{420}-BMC3+ H_2O_2, (III) TPGQD^{420}.

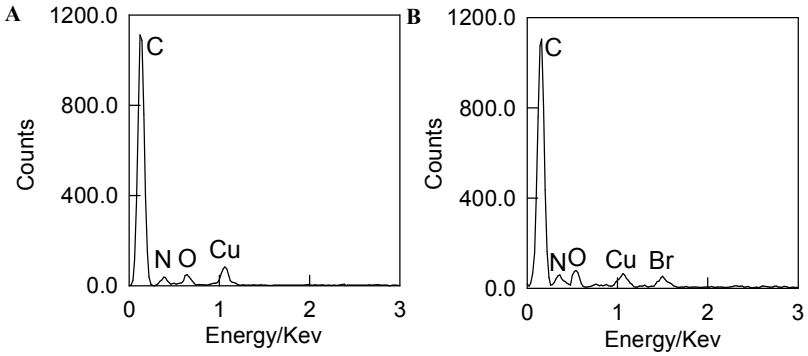

Figure S17. EDX data of TPGQD^{420} (A) and TPGQD^{420}-BMC3 (B).

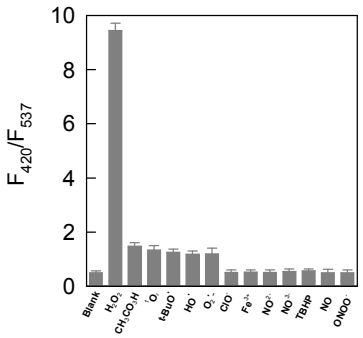

Figure S18. Fluorescence responses of TPGQD^{420}-BMC3 (7.2 μg mL^{-1}) treated by various kinds of reactive oxygen species (ROS). Plot of R= F_{420}/F_{537} as a function of the ROS at 40 μM. Data were acquired in PBS buffer (20mM, 10% DMF, pH=7.4).

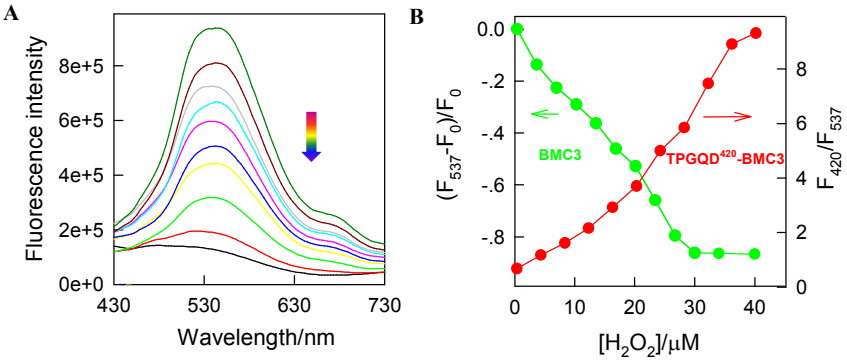

Figure S19. (A) Fluorescence spectra of 360 μM BMC3 in PBS buffer solution (20mM, 10% DMF, pH=7.4) upon addition of different concentrations of H_2O_2. The down arrow indicates the signal changes with the increases in H_2O_2 concentration (0.4, 3.0, 6.0, 10.0, 13.0, 16.0, 20.0, 23, 26, 30 μM). (B) The fluorescence response of BMC3 (Green line) and TPGQD^{420}-BMC3 (Red line) treated by the different concentrations of H_2O_2.

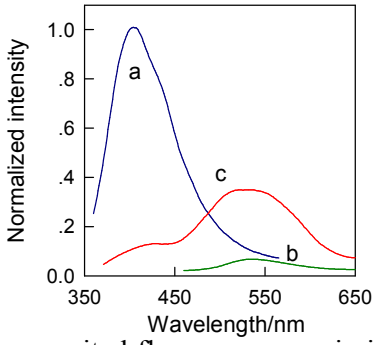

Figure S20. Normalized two-photon excited fluorescence emission spectra of TPGQD^{420} (a), BMC3 (b) and the TPGQD^{420}-BMC3 conjugates (c) in PBS buffer solution (20mM, 10%

DMF, pH=7.4). λ_{ex}= 740 nm.

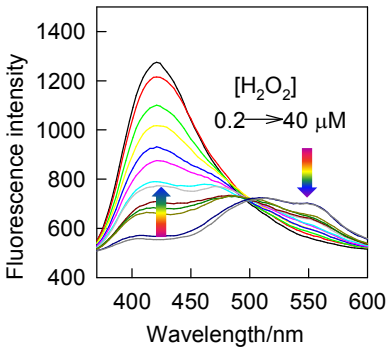

Figure S21. Two-photon excited fluorescence emission spectra for the titration of TPGQD^{420}-BMC3 (0.05 μg/mL) treated with different concentration of H_2O_2 (0.2–40 μM). λ_{ex}= 740 nm.

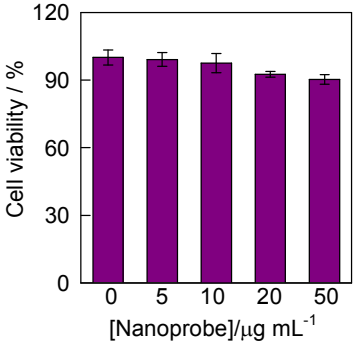

Figure S22. Cell viability of HeLa cells after 24 h treated with different concentrations of TPGQD^{420}-BMC3@PEG at 37 ℃.

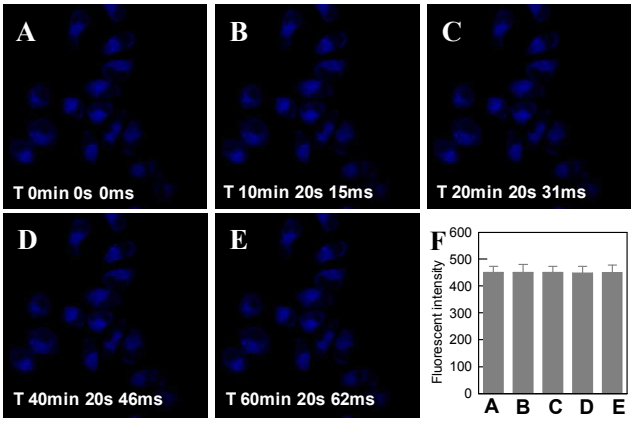

Figure S23. (A–E) Two photon images of HeLa cells treated by TPGQD^{420}-BMC3@PEG in the presence of H_2O_2 were recorded with 600 sec intervals for the duration of one hour using xyt mode under continuous irradiation by the fs-pulses. (F) Quantification and comparison of the relative fluorescence intensity of parts A−E correspondingly. Each data was obtained from

cells in the scanned area and collected in blue channel (400-450 nm).

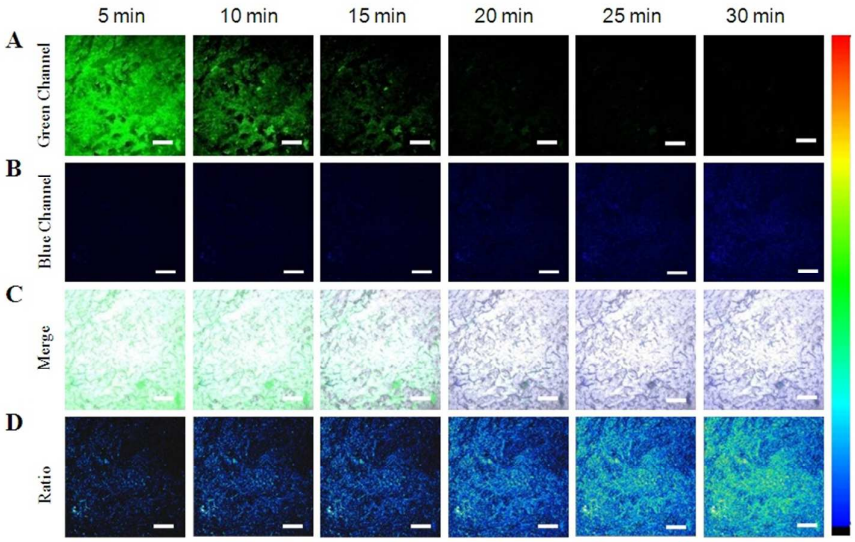

Figure S24. Ratiometric two-photon microscopy images (F_{blue}/F_{green}) of cervical tumor tissue slice stained with TPGQD^{420}-BMC3@PEG at different times. The fluorescence signals were collected in two channels: blue channel (A, 400-450 nm) and green channel (B, 500-550 nm) upon excitation at 740 nm. The (C) row exhibits the corresponding composite images between bright field and two channels. The ratio images in the (D) row were acquired by Image-Pro Plus software. Scale bars: 200 mm.

Synthesis

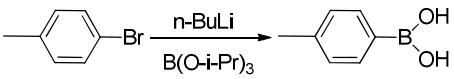

Preparation of p-tolylboronic acid In a typical procedure an oven-dried 250 mL two-neck round bottomed flask with magnetic stirrer was equipped with a rubber septum and allowed to cool under a dry nitrogen atmosphere. Dry THF (125 mL) was then added via cannulation. 1-bromo-4-methylbenzene, purified via passing neat through a short plug of neutral alumina (Brockmann I, 50-200 μm) prior to use (7.18 g, 5.17 mL, 42.0 mmol) was then injected into the flask, and the stirred solution was cooled to -78 °C . After 10 minutes a solution of

n-butyllithium (16.8 mL, 2.5 M in hexanes, 42 mmol) was added dropwise over a period of 10 minutes. The solution was then allowed to warm slightly to ensure thorough mixing of the lithium salts, and stirred at -78 °C for a further 1.5 hours. Triisopropyl borate (9.70 mL, 42.0 mmol) was then added dropwise over 10 minutes, after which the solution was stirred for a further 1.5 hours before being allowed to warm to approximately 0 – 10 °C, whereupon water (10 mL) was added slowly. The resultant solution was then partitioned between water (100 mL), saturated aqueous NH_4Cl (15 mL), and diethyl ether (75 mL). The organic components were separated and the aqueous layer washed with further diethyl ether (3 × 50 mL). The organic layers were combined, dried ($MgSO_4$), and concentrated in vacuo. The resultant solid was further dried in a vacuum dessicator for 1-2 hours, to generate the title compound as a white to off-white powder (4.85 g, 85% yield), which was used without further purification. ^{1}H NMR (400MHz, $CDCl_3$): δ□ □8.13 (d, *J* = 7.7 Hz, 2H), 7.32 (d, *J* = 7.7 Hz, 2H), 2.45 (s, 3H); ^{13}C NMR (100MHz, $CDCl_3$): δ 143.1, 135.9, 128.9, 22.1; ESI-HRMS (m/z): calcd for $C_7H_8BO_2$ [M]+ 135.96, found: 136.2

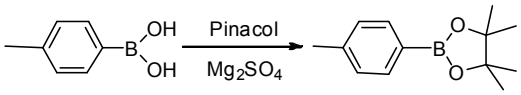

Preparation of 4,4,5,5-tetramethyl-2-p-tolyl-1,3,2-dioxaborolane In a typical procedure, to a 100 mL round bottom flask fitted with a magnetic stirrer was added ptolylboronic acid (4.89 g, 36.0 mmol), anhydrous pinacol (4.68 g, 39.6 mmol), and diethyl ether (50 mL). After stirring for 5 minutes $MgSO_4$ (5g) was added and the flask sealed with a rubber septum. The reaction was stirred vigorously overnight at room-temperature, the solids were then removed by filtration, and washed with diethyl ether (3 × 25 mL). The crude filtrate was then

concentrated in vacuo and redissolved in petrol, before being passed through a plug of silica slurried with petrol. The silica was washed with further portions of petrol and the resultant solution was concentrated in vacuo and thoroughly dried under vacuum to generate the title compound as a white crystalline solid (7.81 g, 99.5% yield) which was used without further purification. If necessary the product was forced to crystallise by cooling the flask briefly on a bed of dry-ice. ^{1}H NMR (400MHz, $CDCl_3$): δ 7.76 (d, J = 8.0 Hz, 2H), 7.22 (d, J = 8.2 Hz, 2H), 2.40 (s, 3H), 1.37 (s, 12H); ^{13}C NMR (100MHz): δ 141.4, 134.9, 128.6, 83.7, 25.0, 21.8; ESI-HRMS (m/z): calcd for $C_{13}H_{19}BO_2$ $[M]^+$ 218.10, found: 218.20

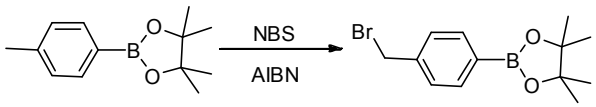

1

Preparation of 2-(4-(bromomethyl)phenyl)-4,4,5,5-tetramethyl-1,3,2-dioxaboro lane (1) In a typical procedure, to a 500 mL round bottom flask fitted with a magnetic stirrer was added 4,4,5,5-tetramethyl-2-p-tolyl-1,3,2-dioxaborolane (7.42 g, 34.0 mmol), N-bromosuccinimide (6.05 g, 34.0 mmol), and acetonitrile (250 mL). The solution was stirred for 5 minutes prior to the addition of AIBN (112 mg, 0.68 mmol, 2 mol%). A condensor was then fitted to the flask and the solution refluxed at 90 °C for 4 hours under an air atmosphere. After cooling to room temperature the solution was concentrated on a rotary evaporator, using two portions of ethyl acetate (75 mL) to azeotropically remove the remaining acetonitrile. The crude material was then slurried with petrol (25 mL) and filtered through a plug of silica, eluting with petrol. The resulting solution was then concentrated in vacuo, and dried under high vacuum if necessary. The crystalline product that formed was then washed with a small

amount of petrol and recrystallised from minimal petrol to generate the title compound as large colourless crystals (7.17 g, 71% yield). Careful recrystallization of the retained mother-liqours and washes yielded further product upon concentration and cooling (0.92 g, 9% yield; total 80% yield). ^{1}H NMR (400MHz, $CDCl_3$):δ 7.79 (d, *J* = 8.2 Hz, 2H) 7.39 (d, *J* = 8.2 Hz, 2H), 4.49 (s, 2H) 1.34 (s, 12H); ^{13}C NMR (100MHz, $CDCl_3$): δ 140.8, 135.4, 128.4, 84.0, 33.4, 25.0; EI-MS (m/z): calcd for $C_{13}H_{18}BBrO_2$ $[M]^+$ 297.00, found: 297.20

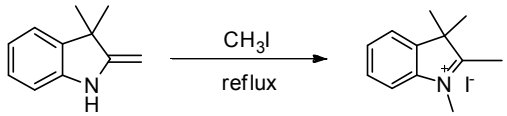

Preparation of N-Methyl-2, 3, 3-trimethylindolenine. In a typical procedure, to a 100 mL round bottom flask a mixture of 2,3,3-trimethylindolenine (0.79 g, 5.0 mmol) and iodomethane (0.85 g, 0.61 mmol) was heated to 50 °C for 2 h under N_2. After cooling the solution to room temperature, yellow crystals were collected by filtration. The solid was washed with ethanol and diethyl ether successively. The solvent was removed under vacuum, and the residue was recrystalized from absolute ethanol to give the product (1.05 g, 70% yield) ^{1}H NMR (400MHz, DMSO): δ 7.92 (m, 1H), 7.83 (dd, *J* = 2, 1H), 7.62 (dd, *J* = 2.8, 2H), 2.97 (s, 3H), 2.77 (s, 3H), 1.53 (s, 6H). ^{13}C NMR (100MHz, DMSO): δ 196.2, 142.3, 141.8, 129.5, 129.0, 123.5, 115.4, 54.2, 35.0, 21.9, 14.5. EI-MS (m/z): calcd for $C_{12}H_{16}N$ $[M]^+$ 174.26, found: 174.00

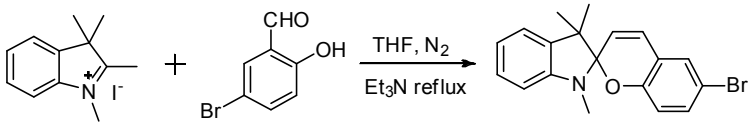

Preparation of SP-Br. 1,2,3,3-tetramethyl-3H-indol-1-ium iodide (335 mg, 1.11 mmol) was dissolved in freshly distilled EtOH (10 mL) and anhydrous Et_3N (200 μL, 1.43 mmol). 5-bromo-2-hydroxybenzaldehyde (220 mg, 1.09 mmol) was added and the reaction mixture was stirred under argon for 3 hours under reflux. After 3 h the solvent was removed under reduced pressure, the residue was dissolved in CH_2Cl_2 and dried over anhyd Na_2SO_4. The solvent was evaporated under reduced pressure, and the residue was dried in vacuo and purified by gradient flash chromatography on silica gel to the product as a pale pink solid (300 mg, 77% yield). ^{1}H NMR (400MHz, $CDCl_3$): δ 7.15–7.27 (m, 3H), 7.09 (d, *J* = 7.2 Hz,1H), 6.87 (t, *J* = 7.4 Hz,1H), 6.80 (d, *J* = 10.3 Hz, 1H), 6.61 (d, *J* = 9.2 Hz, 1 H), 6.55 (d, *J* = 7.7 Hz,1 H), 5.74 (d, *J* = 10.2 Hz, 1H), 2.74 (s, 3H), 1.32 (s, 3H), 1.18 (s, 3H). ^{13}C NMR (100MHz, $CDCl_3$): 153.6, 148.0, 136.5, 132.2, 129.1, 128.4, 127.7, 121.5, 120.7, 120.6, 119.3, 116.9, 111.8, 106.9, 104.5, 51.9, 28.9, 25.9, 20.1. EI-MS (m/z): calcd for $C_{19}H_{18}BrNO$: 356.26; found: 357.00.

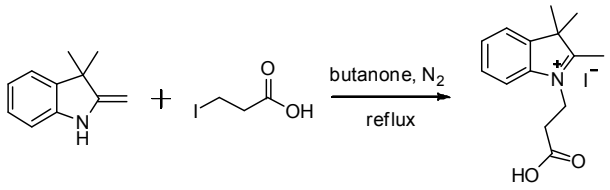

Preparation of 1-(2-carboxyethyl)-2,3,3-trimethyl-3H-indol-1-ium iodide: 2,3,3-trimethylindolenine (5.01 mL, 30.59 mmol) and 3-iodopropanic acid (6.35 g, 30.17 mmol) were diluted in 10 mL butanone and stirred under argon for 5 hours under reflux. The precipitate was suspended in 50 mL H_2O and washed three times with 50 mL DCM. The organic layers were combined and washed three times with 25 mL water. The aqueous layers were combined, filtered and the solvent removed at high vacuum, receiving the product as

pale yellow solid (10.52 g, 97 % yield). ^{1}H NMR (400MHz, DMSO): δ 1.55 (s, 6H), 2.89 (s, 3H), 3.00 (t, *J* = 6.88 Hz, 2H), 4.67 (t, *J* = 6.76 Hz, 2H), 7.64-7.58 (m, 2H), 7.84-7.89 (m, 1H), 7.97-8.03 (m, 1H). ^{13}C NMR (100MHz, DMSO): δ 197.99, 171.66, 141.83, 140.93, 129.43, 129.01, 123.57, 115.65, 54.34, 43.58, 31.17, 21.95, 14.39. EI-MS (m/z): calcd for $C_{14}H_{18}NO_2^+$: 232.30; found: 232.10.

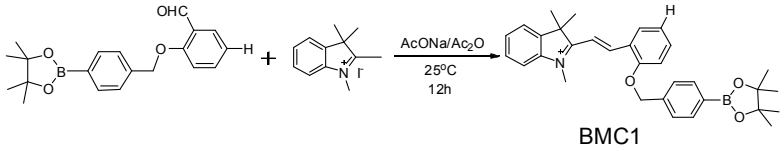

Synthesis of BMC1.A mixture of 2-((4-(4,4,5,5-tetramethyl-1,3,2-dioxaborolan-2-yl) benzyl)oxy)benzaldehyde (0.067mmol), 1,2,3,3-tetramethyl-3H-indolium iodide (0.2994g, 0.0994mmol) and sodium acetate (0.0816g, 0.0994mmol) was reacted in acetic anhydride (20mL) according to general procedure to give BMC1 (89%) as a dark brown solid.^{1}H NMR(400MHz, $CDCl_3$): δ 8.45 (d, *J* = 16.5 Hz, 1H), 8.33 (d, *J* = 2.4 Hz, 1H), 7.87 (d, *J* = 8.1 Hz, 2H), 7.73 (d, *J* = 16.5 Hz, 1H), 7.65 (dd, *J* = 5.9, 3.1 Hz, 1H), 7.60 (d, *J* = 2.4 Hz, 1H), 7.58 – 7.55 (m, 2H), 7.54 – 7.50 (m, 2H), 7.47 (d, *J* = 8.0 Hz, 2H), 6.97 (d, *J* = 8.9 Hz, 1H), 5.21 (d, *J* = 6.5 Hz, 2H), 4.31 (s, 3H), 1.76 (s, 6H), 1.36 (s, 12H). ^{13}C NMR (100MHz, $CDCl_3$): δ 182.65, 158.97, 149.58, 142.84, 141.48, 138.81, 136.13, 135.20, 131.54, 129.73, 129.62, 126.75, 123.03, 122.43, 122.37, 114.82, 112.85, 112.52, 84.02, 70.85, 52.28, 36.87, 27.07, 24.86. MS (ESI): m/z calc. for $C_{32}H_{37}BNO_3^+$: 494.45; found: 494.2 $[M]^+$

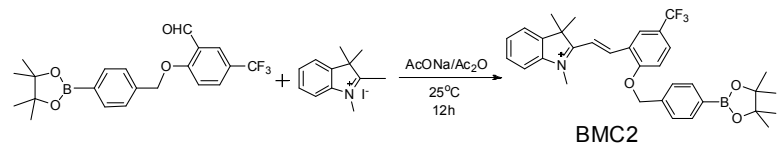

Synthesis of BMC2.A mixture of 2-((4-(4,4,5,5-tetramethyl-1,3,2-dioxaborolan-2-yl) benzyl)oxy)-5-(trifluoromethyl)benzaldehyde(0.067mmol),1,2,3,3-tetramethyl-3H-indolium iodide (0.2994g, 0.0994mmol) and sodium acetate (0.0816g, 0.0994mmol) was reacted in acetic anhydride (20mL) according to general procedure to give BMC2 (43%) as a dark yellow solid.^{1}H NMR(400MHz, $CDCl_3$): δ 8.45 (d, *J* = 16.0 Hz, 1H), 8.25 (s, 1H), 7.90 (d, *J* = 7.4 Hz, 2H), 7.79 (d, *J* = 20.1 Hz, 2H), 7.64 (s, 1H), 7.60 (s, 2H), 7.53 (d, *J* = 7.1 Hz, 3H), 7.19 (d, *J* = 9.1 Hz, 1H), 5.31 (s, 2H), 4.25 (s, 3H), 1.80 (s, 6H), 1.38 (s, 12H).^{13}C NMR (100 MHz, $CDCl_3$):δ 182.96, 157.63, 147.41, 143.32, 141.86, 138.69, 135.57, 135.32, 130.35, 129.98, 127.85, 127.14, 124.58, 122.78, 115.49, 114.70, 114.41, 84.36, 71.64, 57.28，52.86, 37.32, 27.23, 25.19. MS (ESI): m/z calc. for $C_{33}H_{36}BF_3NO_3^+$: 562.45; found: 562.2 $[M]^+$

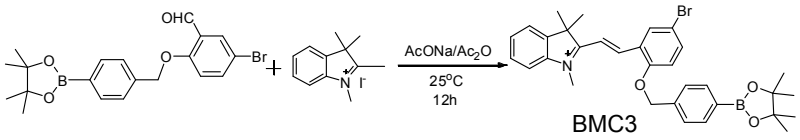

Synthesis of BMC3 A mixture of 5-bromo-2-((4-(4,4,5,5-tetramethyl-1,3,2-Dioxaborolan-2-yl)benzyl)oxy)benzaldehyde(0.067mmol),1,2,3,3-tetramethyl-3H-indoliumio dide (0.2994g, 0.0994mmol) and sodium acetate (0.0816g, 0.0994mmol) was reacted in acetic anhydride (20mL) according to general procedure to give BMC3 (83%) as a yellow solid.^{1}H NMR(400MHz, $CDCl_3$): δ 8.45 (d, *J* = 16.5 Hz, 1H), 8.33 (d, *J* = 2.4 Hz, 1H), 7.87 (d, *J* = 8.1 Hz, 2H), 7.73 (d, *J* = 16.5 Hz, 1H), 7.65 (dd, *J* = 5.9, 3.1 Hz, 1H), 7.60 (d, *J* = 2.4 Hz, 1H), 7.58 – 7.55 (m, 2H), 7.54 – 7.50 (m, 1H), 7.47 (d, *J* = 8.0 Hz, 2H), 6.97 (d, *J* = 8.9 Hz, 1H), 5.21 (d, *J* = 6.5 Hz, 2H), 4.31 (s, 3H), 1.76 (s, 6H), 1.36 (s, 12H). ^{13}C NMR(100MHz, $CDCl_3$): δ 182.91, 158.11, 147.32, 141.95, 138.20, 135.57, 133.22, 130.36, 129.99, 125.04, 122.79,

115.73, 115.54, 114.86, 114.67, 84.35, 71.61, 52.86, 37.33, 27.23, 25.19. MS (ESI): m/z calc. for $C_{32}H_{36}BBrNO_3^+$:573.35; found: 574.1 $[M]^+$

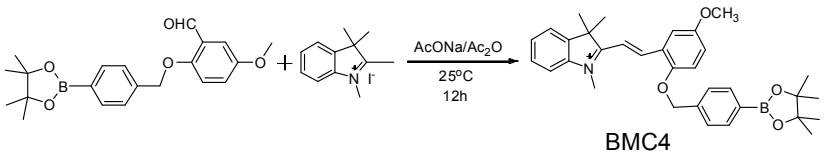

BMC4

Synthesis of BMC4.A mixture of 5-methoxy-2-((4-(4,4,5,5-tetramethyl-1,3,2-dioxaborolan-2-yl)benzyl)oxy)benzaldehyde (0.067 mmol), 1,2,3,3-tetramethyl-3H- indolium iodide (0.2994 g, 0.0994 mmol) and sodium acetate (0.0816 g, 0.0994 mmol) was reacted in acetic anhydride (20 mL) according to general procedure to give BMC4 (90%) as a dark brown solid.^{1}H NMR(400MHz, $CDCl_3$): δ 8.69 (d, *J* = 16.4 Hz, 1H), 7.90 – 7.85 (m, 3H), 7.84 (d, *J* = 2.9 Hz, 1H), 7.57 (d, *J* = 1.4 Hz, 2H), 7.56 – 7.53 (m, 2H), 7.51 (d, *J* = 4.6 Hz, 1H), 7.47 (d, *J* = 8.0 Hz, 2H), 7.00 (d, *J* = 9.2 Hz, 1H), 5.18 (s, 2H), 4.39 (s, 3H), 4.06 (s, 3H), 1.73 (s, 6H), 1.37 (s, 12H).^{13}C NMR (100MHz, $CDCl_3$):δ 183.07, 155.01, 154.31, 149.88, 143.25, 141.78, 139.36, 135.51, 129.99, 127.09, 125.24, 123.80, 122.78, 122.58, 114.86, 114.47, 113.17, 112.84, 84.34, 71.76, 58.23, 52.61, 37.51, 27.40, 25.19. MS (ESI): m/z calc. for $C_{33}H_{39}BNO_4^+$: 524.48; found: 524.2 $[M]^+$

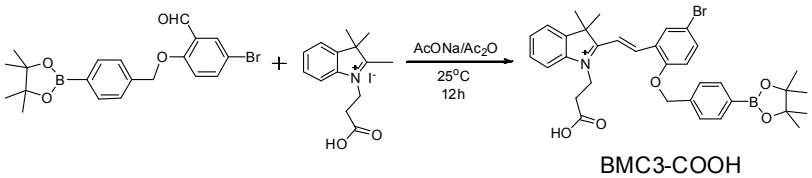

BMC3-COOH

Synthesis of BMC3-COOH. ^{1}H NMR(400MHz, $CDCl_3$): δ 8.45 (d, *J* = 16.5 Hz, 1H), 8.33 (d, *J* = 2.4 Hz, 1H), 7.87 (d, *J* = 8.1, Hz, 2H), 7.73 (d, *J* = 16.5 Hz, 1H), 7.65 (dd, *J* = 5.9, 3.1 Hz, 1H), 7.58 – 7.55 (m, 2H), 7.54 – 7.50 (m, 1H), 7.47 (d, *J* = 8.0 Hz, 2H), 6.97 (d, *J* = 8.9

Hz, 1H), 5.21 (d, J = 6.5 Hz, 1H), 4.31 (s, 2H), 3.72 (t, J = 6.7 Hz, 2H), 3.14 (t, J = 6.7 Hz, 2H), 1.76 (s, 6H), 1.36 (s, 12H). ^{13}C NMR (100 MHz, $CDCl_3$) δ 182.91, 176.62, 158.11, 147.32, 143.31, 141.85, 138.67, 138.20, 135.57, 133.22, 130.36, 129.99, 127.16, 125.04, 122.79, 115.54, 114.89, 114.67, 84.35, 71.61, 52.86, 37.54, 37.33, 27.23, 25.19, 24.96. MS (ESI): m/z calc. for $C_{34}H_{38}BBrNO_5^+$:631.38; found: 630.2 $[M]^+$

^{1}H NMR ^{13}C NMR and HRMS (ESI)

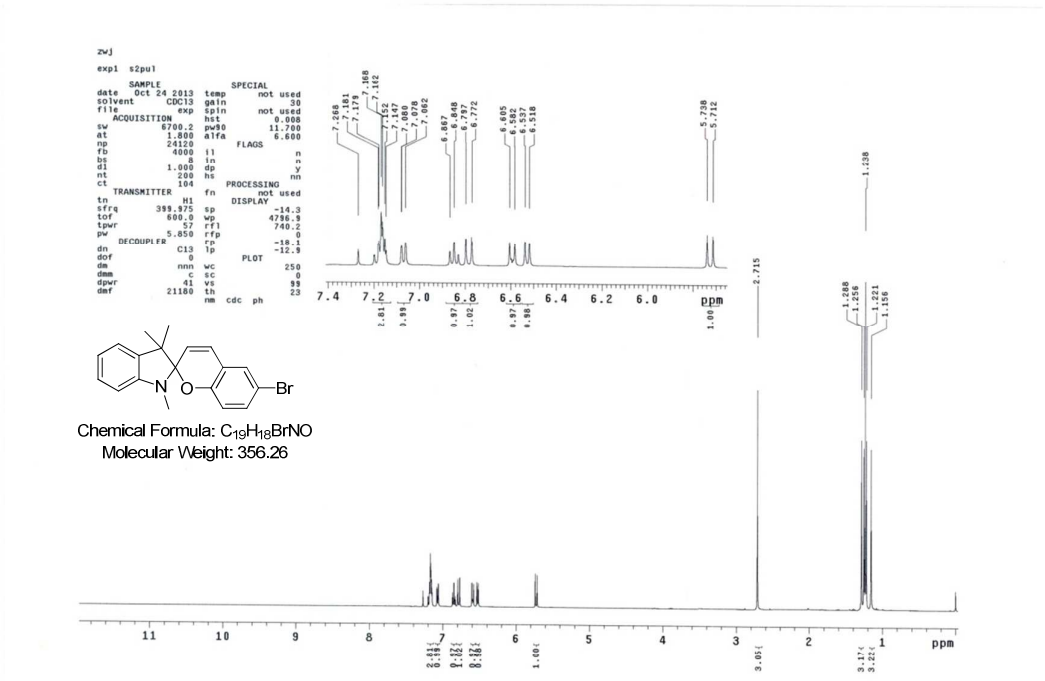

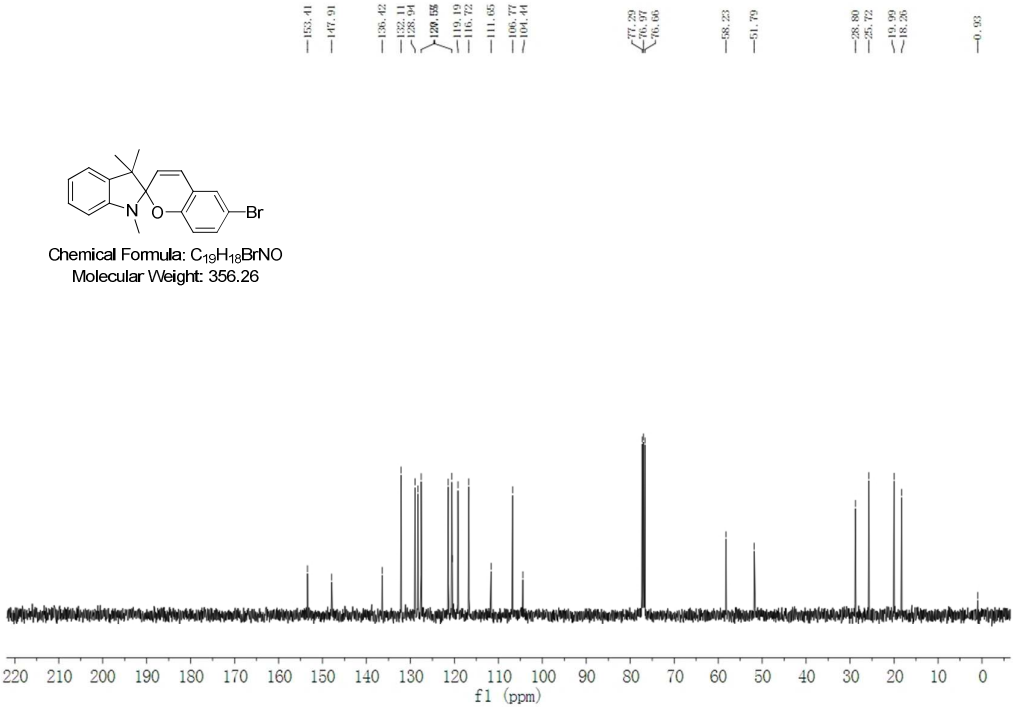
153.41
147.91
136.42
132.11
128.94
120.55
119.19
116.72
111.65
106.77
104.44
77.29
76.97
76.66
58.23
51.79
28.80
25.72
19.99
18.26
0.93
Br
Chemical Formula: C19H18BrNO
Molecular Weight: 356.26
220 210 200 190 180 170 160 150 140 130 120 110 100 90 80 70 60 50 40 30 20 10 0
f1 (ppm)

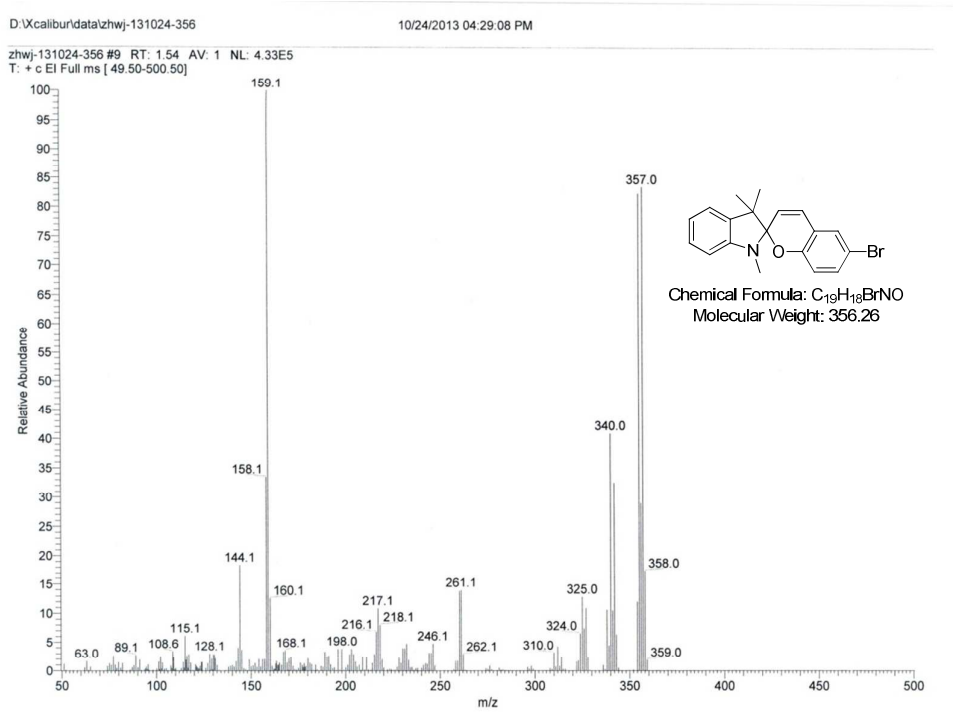
D:\Xcalibur\data\zhwj-131024-356
10/24/2013 04:29:08 PM
zhwj-131024-356 #9 RT: 1.54 AV: 1 NL: 4.33E5
T: + c EI Full ms [49.50-500.50]
Relative Abundance
m/z
159.1
357.0
340.0
158.1
144.1
358.0
160.1
325.0
261.1
217.1
218.1
216.1
324.0
115.1
246.1
359.0
63.0
89.1
108.6
128.1
168.1
198.0
262.1
310.0
Br
Chemical Formula: C19H18BrNO
Molecular Weight: 356.26

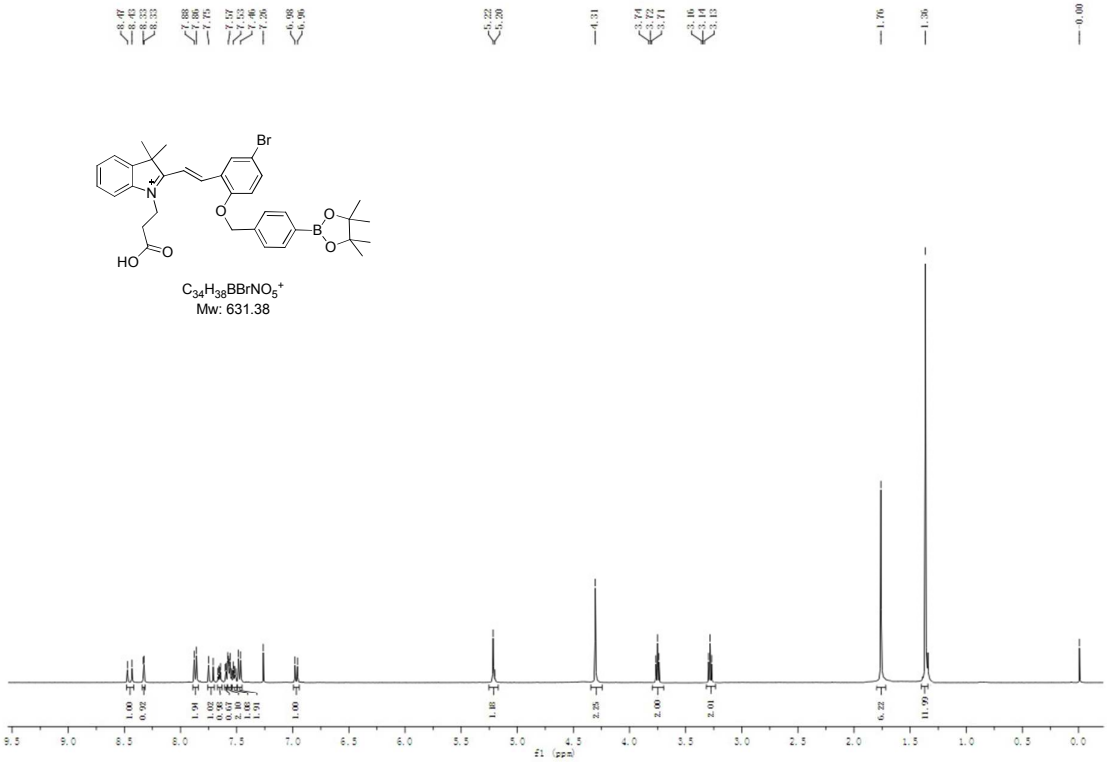

$C_{34}H_{38}BBrNO_5^+$
Mw: 631.38

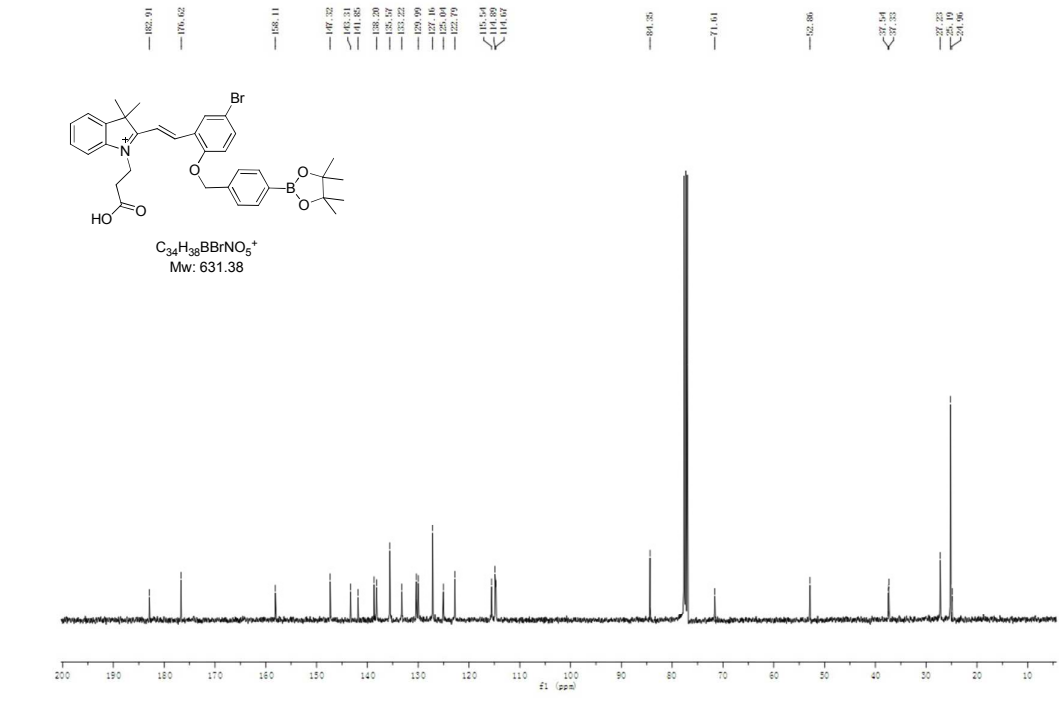

$C_{34}H_{38}BBrNO_5^+$
Mw: 631.38

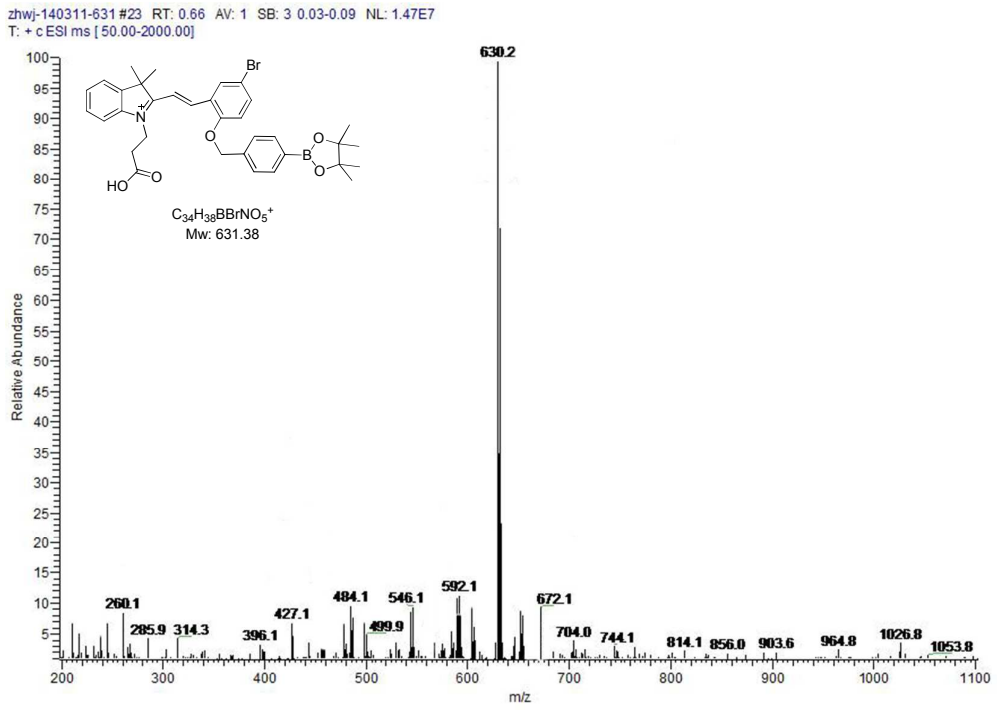
zhwj-140311-631 #23 RT: 0.66 AV: 1 SB: 3 0.03-0.09 NL: 1.47E7
T: + c ESI ms [50.00-2000.00]
Br
HO
O
$C_{34}H_{38}BBrNO_5^+$
Mw: 631.38
Relative Abundance
m/z
630.2
260.1
285.9
314.3
396.1
427.1
484.1
499.9
546.1
592.1
672.1
704.0
744.1
814.1
856.0
903.6
964.8
1026.8
1053.8

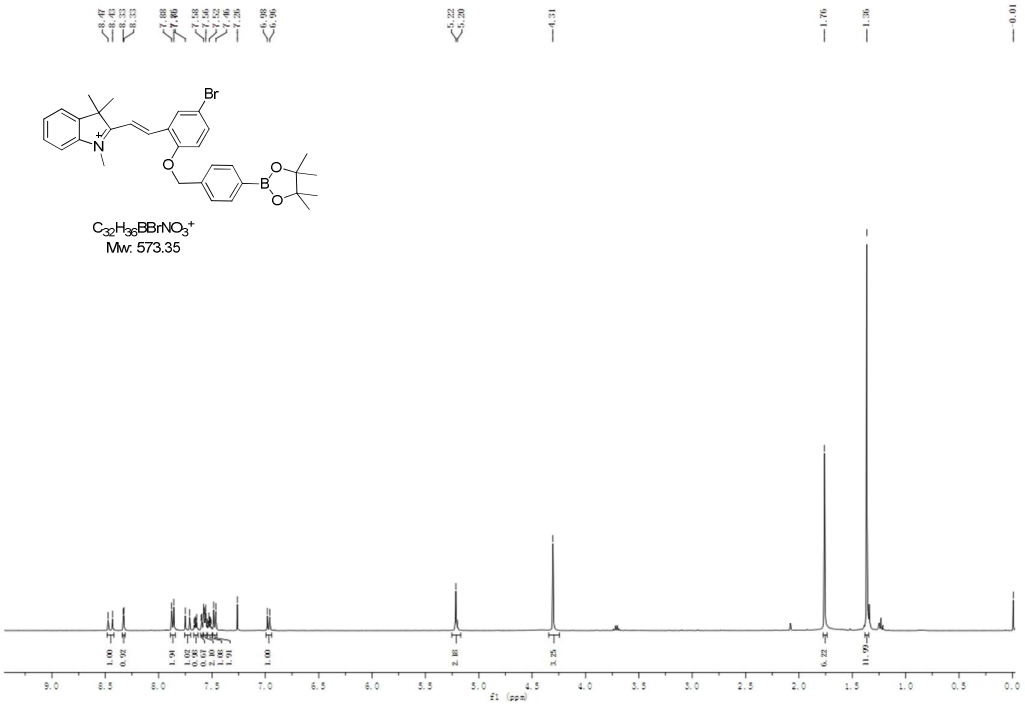
Br
$C_{32}H_{36}BBrNO_3^+$
Mw: 573.35

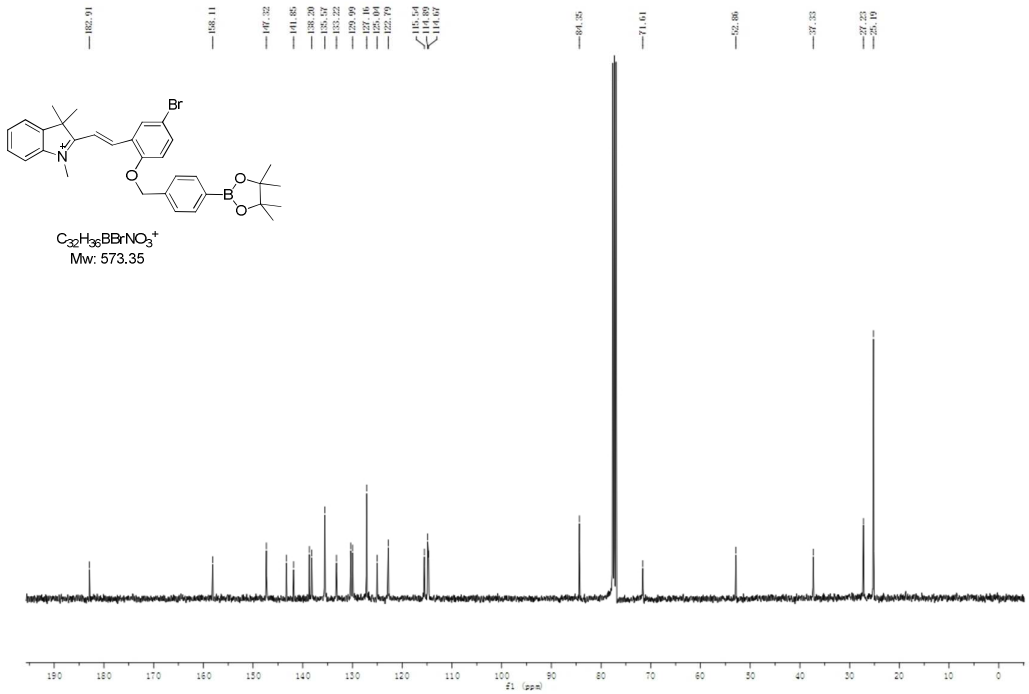
182.91
158.11
147.32
141.85
138.29
135.54
133.22
129.99
127.16
125.80
122.79
115.54
114.89
114.67
84.35
71.61
52.86
37.33
27.23
25.19
Br
O
B
O
O
$C_{32}H_{36}BBrNO_3^+$
Mw: 573.35
190
180
170
160
150
140
130
120
110
100
90
80
70
60
50
40
30
20
10
0
f1 (ppm)

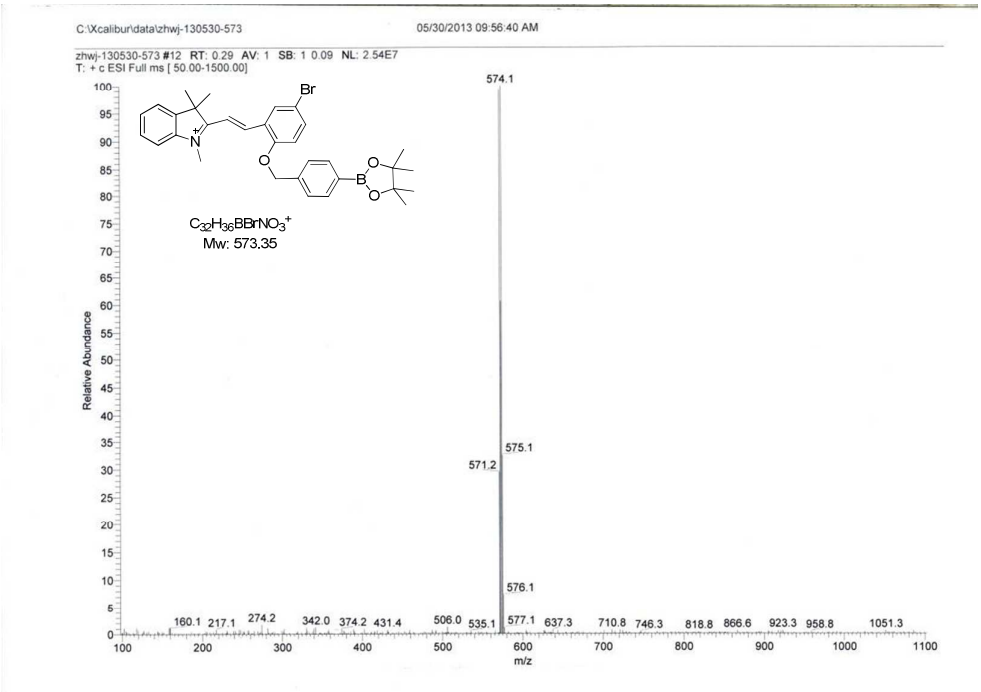
C:\Xcalibur\data\zhwj-130530-573
05/30/2013 09:56:40 AM
zhwj-130530-573 #12 RT: 0.29 AV: 1 SB: 1 0.09 NL: 2.54E7
T: + c ESI Full ms [50.00-1500.00]
Br
O
B
O
O
$C_{32}H_{36}BBrNO_3^+$
Mw: 573.35
Relative Abundance
574.1
575.1
571.2
576.1
160.1
217.1
274.2
342.0
374.2
431.4
506.0
535.1
577.1
637.3
710.8
746.3
818.8
866.6
923.3
958.8
1051.3
m/z

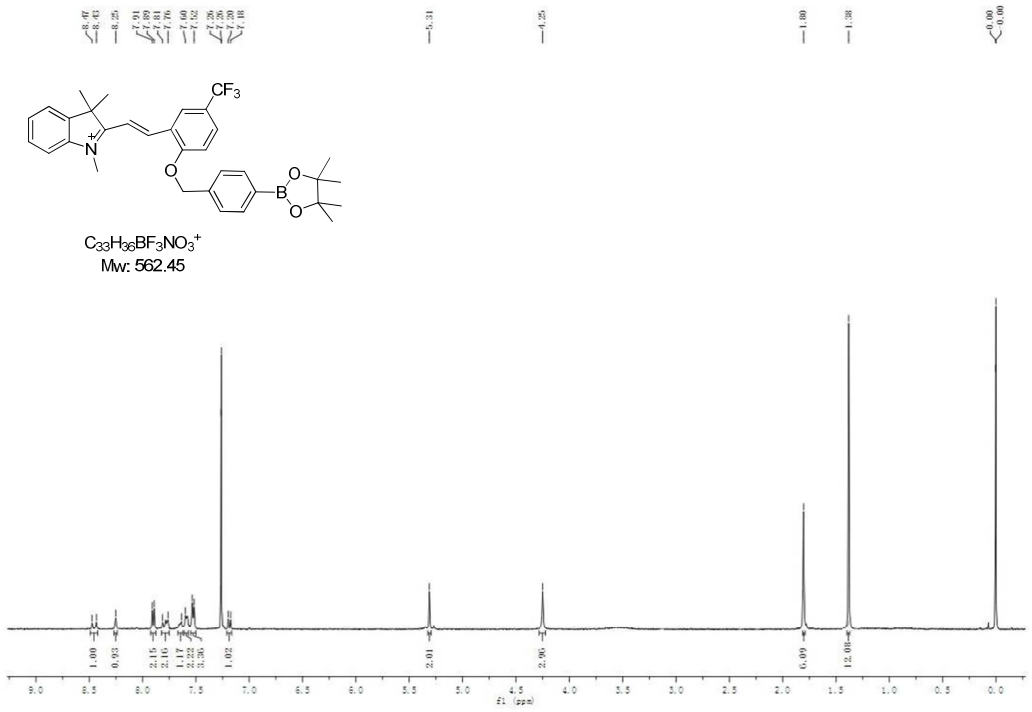
CF3
O
B
O
O
C33H36BF3NO3+
Mw: 562.45
f1 (ppm)

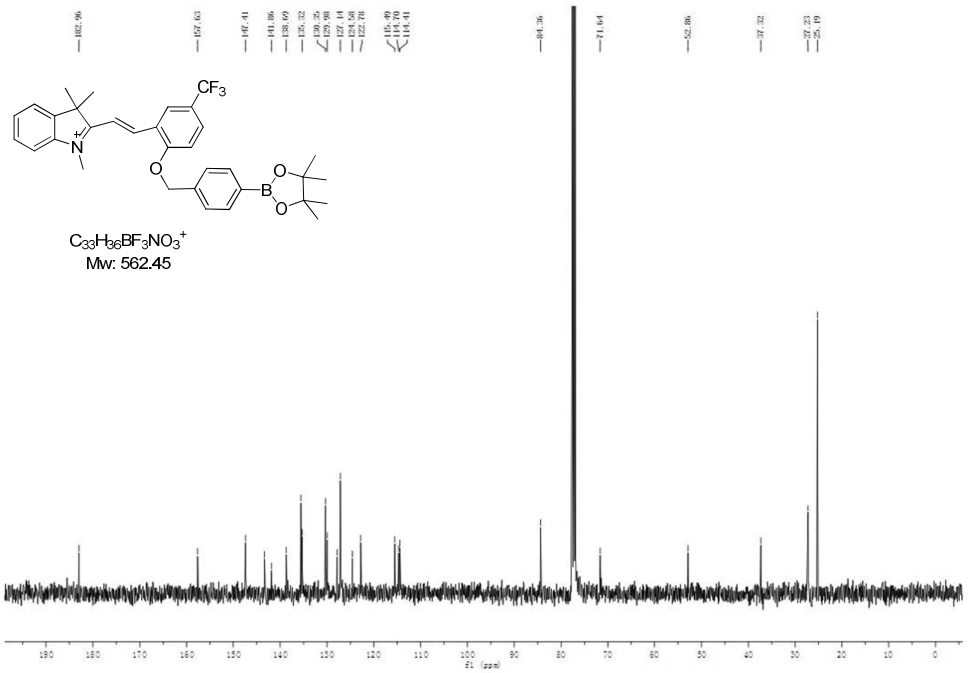
CF3
O
B
O
O
C33H36BF3NO3+
Mw: 562.45
f1 (ppm)

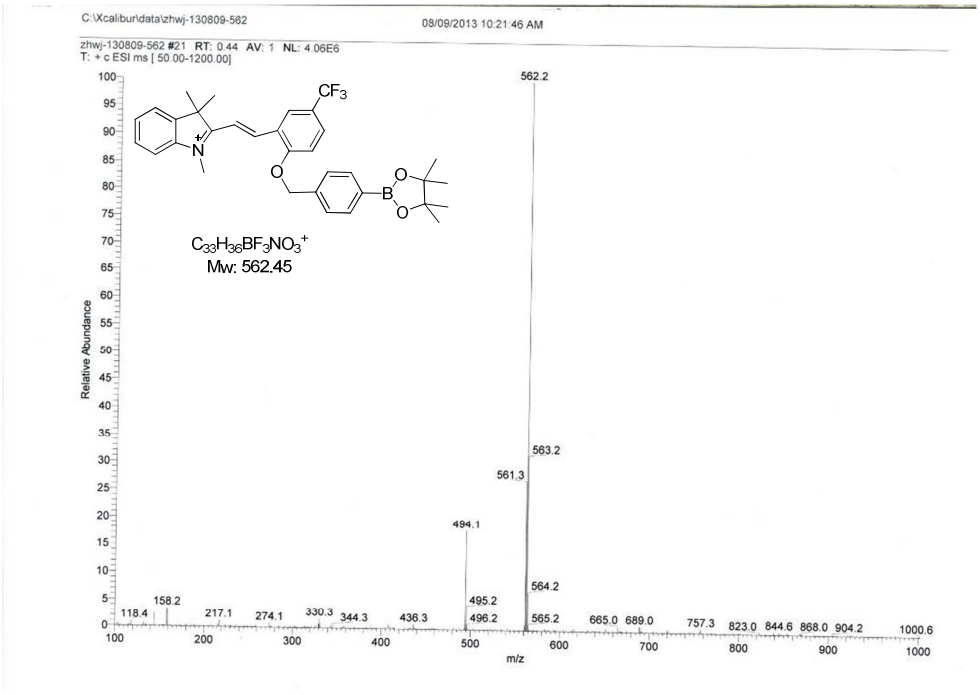
C:\Xcalibur\data\zhwj-130809-562
08/09/2013 10:21:46 AM
zhwj-130809-562 #21 RT: 0.44 AV: 1 NL: 4.06E6
T: + c ESI ms [50.00-1200.00]
CF3
C33H36BF3NO3+
Mw: 562.45
Relative Abundance
m/z
562.2
563.2
561.3
494.1
564.2
158.2
495.2
118.4
217.1
274.1
330.3
344.3
436.3
496.2
565.2
665.0
689.0
757.3
823.0
844.6
868.0
904.2
1000.6

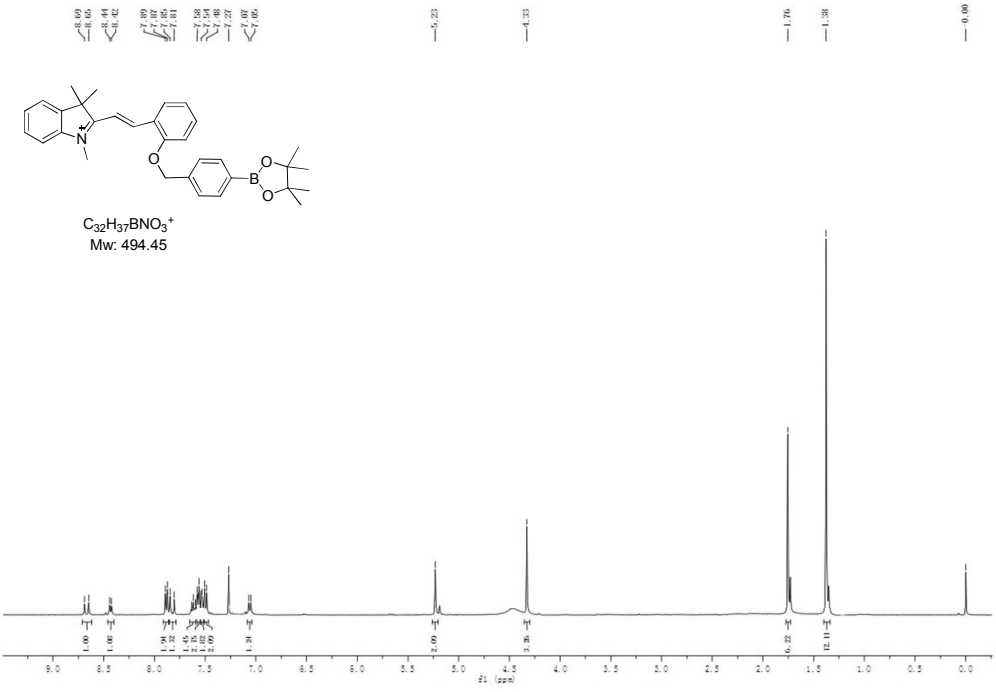
C32H37BNO3+
Mw: 494.45
f1 (ppm)

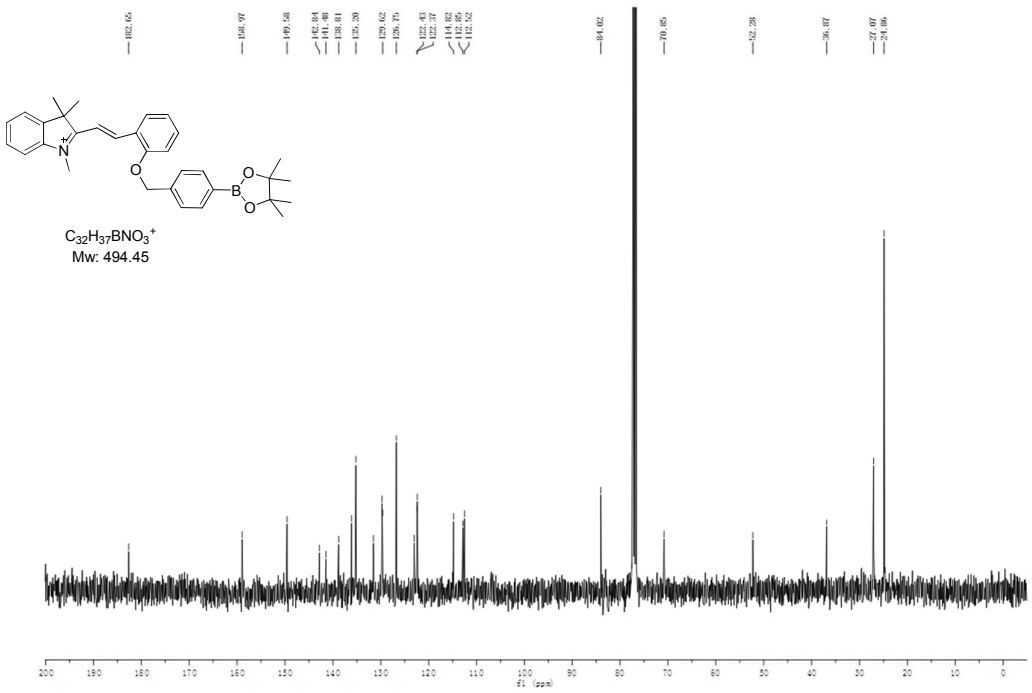
182.65
158.97
149.58
142.84
141.48
138.81
135.20
129.62
126.75
122.43
122.37
114.82
112.95
112.52
84.02
70.85
52.38
26.87
27.07
24.86
C32H37BNO3+
Mw: 494.45
200 190 180 170 160 150 140 130 120 110 100 90 80 70 60 50 40 30 20 10 0
f1 (ppm)

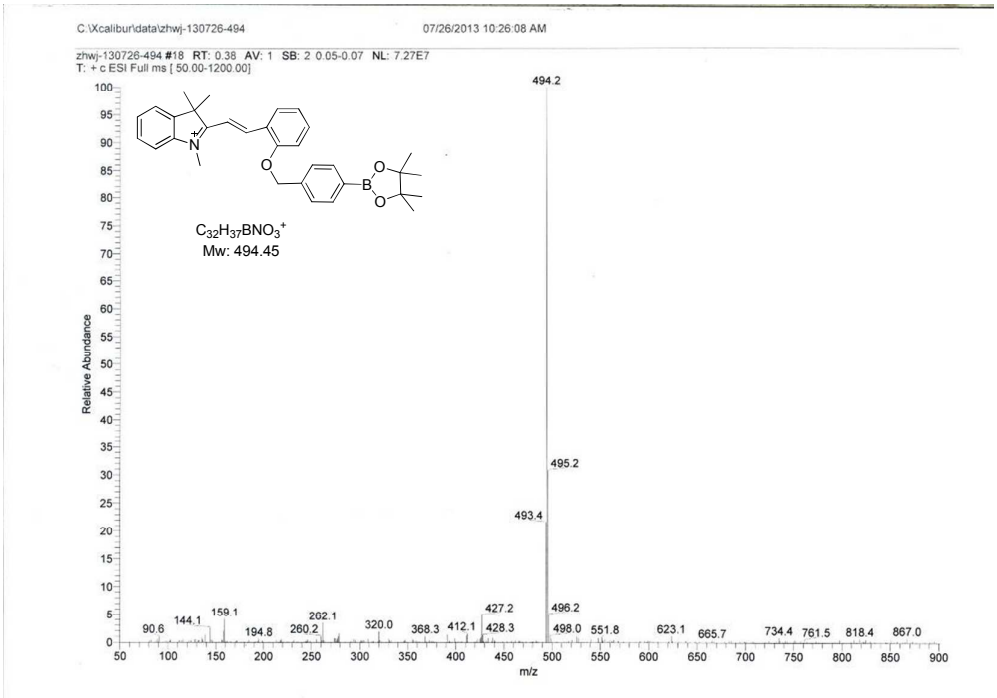
C:\Xcalibur\data\zhwj-130726-494
07/26/2013 10:26:08 AM
zhwj-130726-494 #18 RT: 0.38 AV: 1 SB: 2 0.05-0.07 NL: 7.27E7
T: + c ESI Full ms [50.00-1200.00]
494.2
C32H37BNO3+
Mw: 494.45
Relative Abundance
495.2
493.4
496.2
427.2
159.1
144.1
202.1
90.6
194.8
260.2
320.0
368.3
412.1
428.3
498.0
551.8
623.1
665.7
734.4
761.5
818.4
867.0
m/z

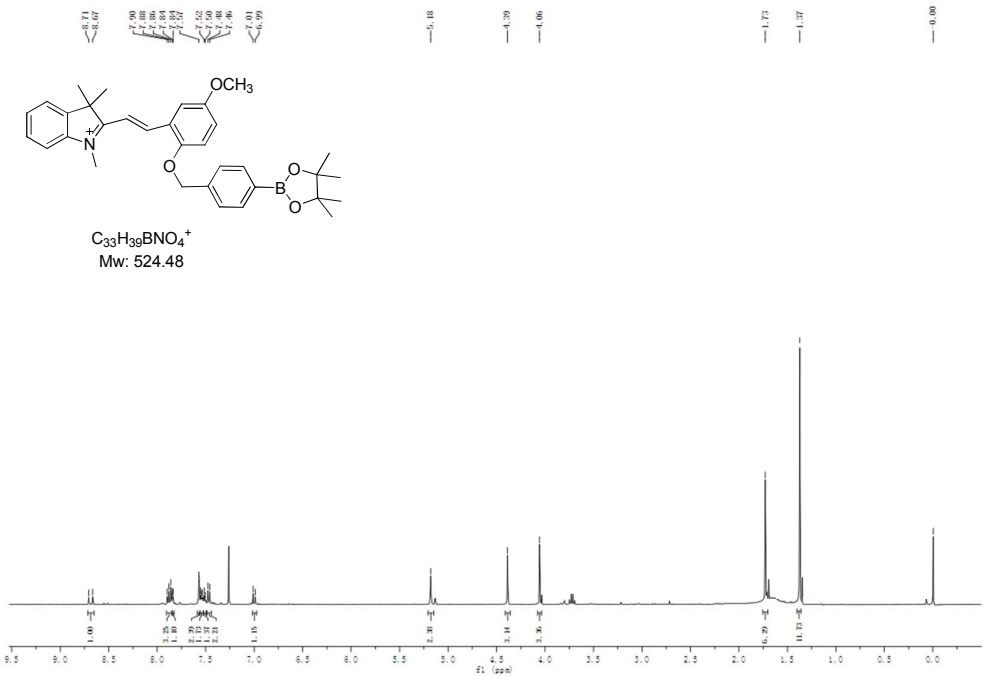
OCH3
N+
O
B
O
O
C33H39BNO4+
Mw: 524.48

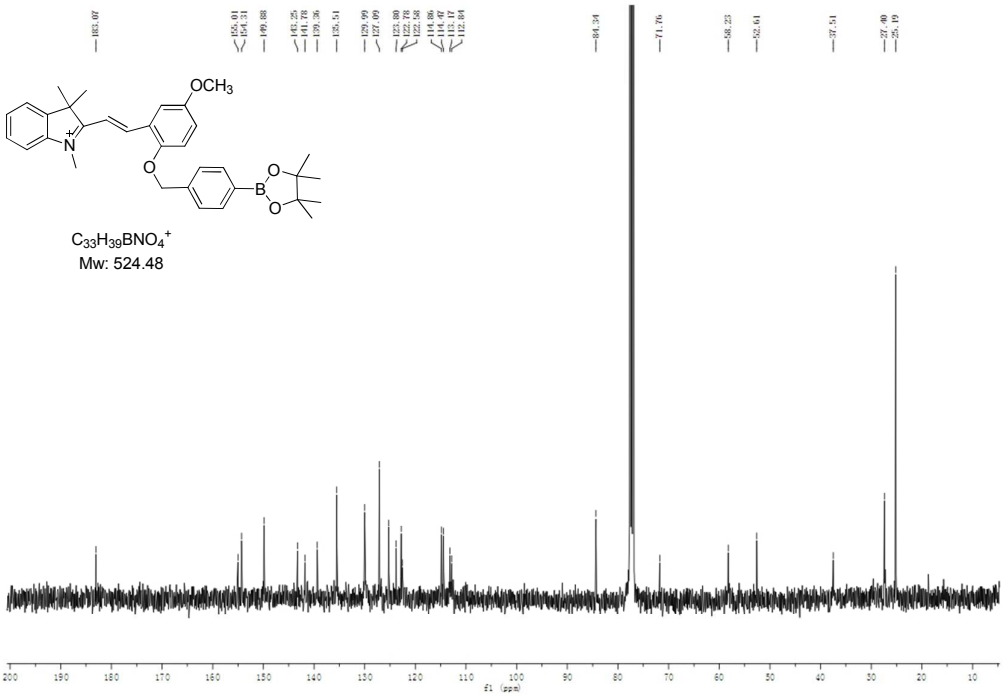
OCH3
N+
O
B
O
O
C33H39BNO4+
Mw: 524.48

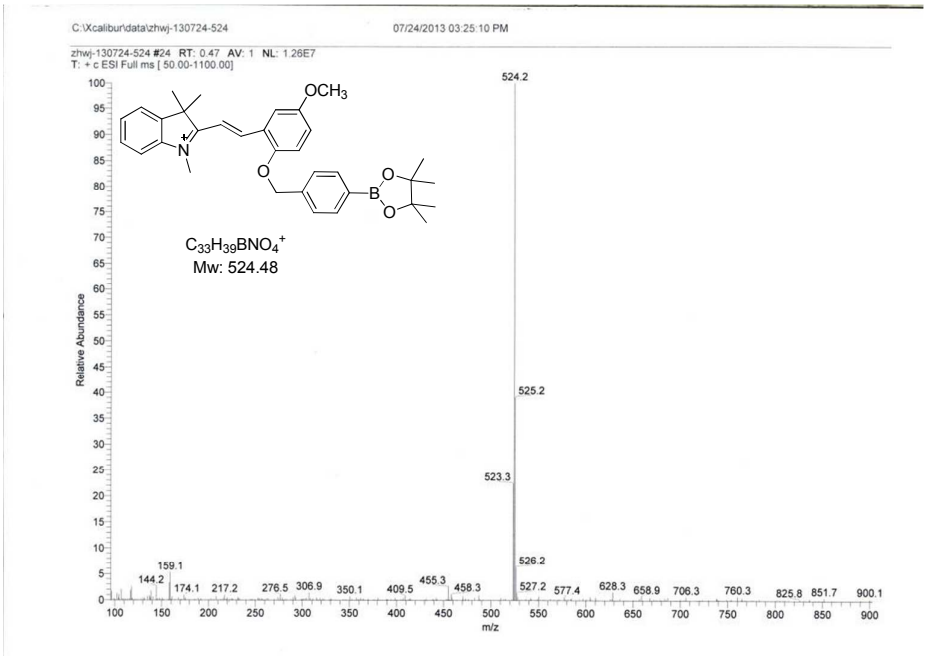
C:\Xcalibur\data\zhwj-130724-524
07/24/2013 03:25:10 PM
zhwj-130724-524 #24 RT: 0.47 AV: 1 NL: 1.26E7
T: + c ESI Full ms [50.00-1100.00]
OCH3
C33H39BNO4+
Mw: 524.48
Relative Abundance
m/z
524.2
525.2
523.3
526.2

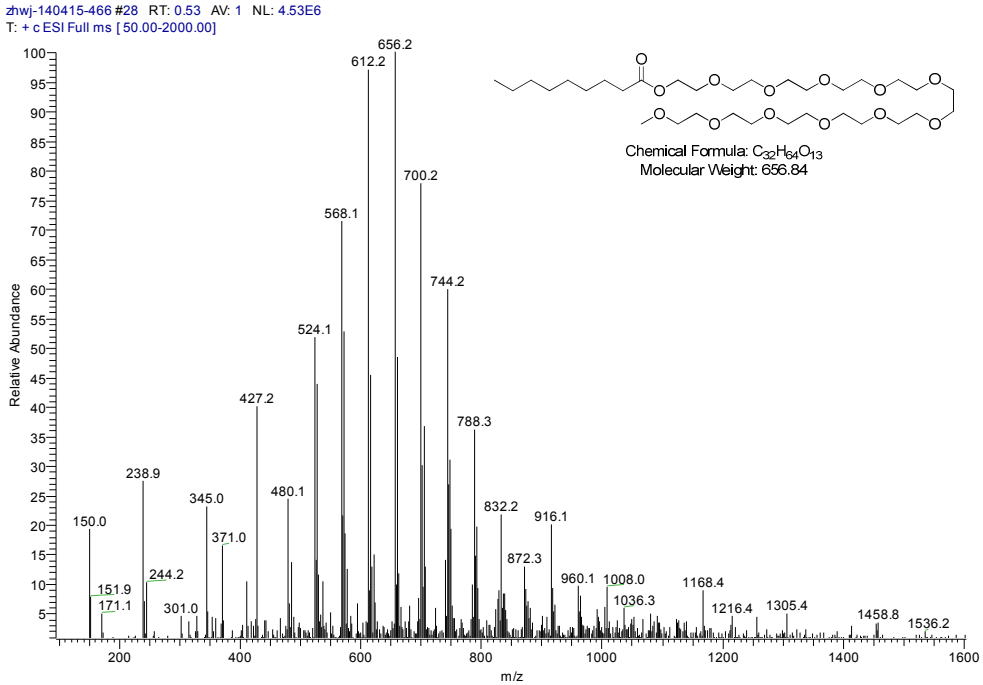
zhwj-140415-466 #28 RT: 0.53 AV: 1 NL: 4.53E6
T: + c ESI Full ms [50.00-2000.00]
Chemical Formula: C32H64O13
Molecular Weight: 656.84
Relative Abundance
m/z
656.2
612.2
700.2
568.1
744.2
524.1
427.2
788.3
238.9
345.0
480.1
832.2
916.1
150.0
371.0
872.3
244.2
960.1
1008.0
1168.4
151.9
171.1
301.0
1036.3
1216.4
1305.4
1458.8
1536.2